KINETICS OF TIO2 PHOTOCATALYTIC DECOMPOSITION

KINETICS OF TIO2 PHOTOCATALYTIC DECOMPOSITION

By

RUILIN LI, B. ENG

A Thesis

Submitted to the School of Graduate Studies

in Partial Fulfillment of the Requirements

for the Degree

Master of Applied Science

McMaster University

MASTER OF APPLIED SCIENCE (2008) **McMaster University**

(Chemical Engineering) **Hamilton, Ontario**

TITLE: **Kinetics of TiO_2 Photocatalytic Decomposition**

AUTHOR: **Ruilin Li**

B. Eng. (Zhejiang University)

SUPERVISOR: **Professor Robert H. Pelton**

NUMBER OF PAGES: x, 78

Abstract

Our work demonstrates the decomposition results obtained using TiO_2 coated paper at different pH, ionic strength, UV intensities, temperature and flow rates. A kinetic model of TiO_2 photocatalytic decomposition of reactive azo dye (RB5) was developed for the different conditions.

TiO_2 coated paper was developed by simply spraying TiO_2 suspension on the filter paper. The stability of the TiO_2 coated paper was studied and the environment where TiO_2 coated paper can be used is under pH 7. The stability of TiO_2 attached on the paper surface is determined by the property of the polymeric retention aids and the adsorption of reactive azo dye (RB5) is dependent on the electrostatic attraction.

TiO_2 photocatalytic decomposition mainly occurs at the surface of TiO_2. So the adsorption of RB5 molecules is considered to be one of the most important factors, which can affect the decomposition rate. Other factors, such as UV intensity and temperature, can also change the decomposition rate by affecting the formation of free radicals.

New discovery of intermediate products can make the mechanism of the photocatalytic decomposition more clear, although the specific information about the intermediate products is not available yet. The

adsorption and decomposition of intermediate products provide useful information for developing the decomposition kinetic model.

Langmuir adsorption model is fit for the adsorption of RB5 and its degradation intermediate products at TiO_2 surface. Our kinetics model combines the principles of Langmuir-Hinshelwood model and two-step first-order model. It can describe the change of the RB5 concentration in the bulk and predict the desorption of intermediate products.

Acknowledgments

I believe some steps can lead to the success in my life and the two-year graduate life is one. I am so grateful to the people who let me enjoy the important experience, knowledge and life here.

Firstly, I wish to thank my parents, Xingjian Li and Guixun Xue, who always give me their care, encouragement, support and love since I was born in this world. I love you both.

I would like to thank my supervisor Dr. Robert H. Pelton. He provided me the opportunity to be a graduate student. In these two years, he shared his priceless experiences and knowledge with me and inspired me in my life and work. I want to thank Dr. Carlos Filipe, who always provided guidance and advice like another supervisor for me. Special acknowledgments and thanks go to Dr. Shiping Zhu, who gave a high valued recommendation to let me enter this university and enjoy the graduate life.

I am so grateful for the funding and supports from Sentinel Bioactive Paper Network. I would like to thank all the members in Sentinel Bioactive Paper Network. I got a lot of idea from your work.

I would like to thank Dr. Lily Geng, for her research experiences which lead to a good start for my project; to Dr. Chengming Li, for his

suggestion in my research. Great thanks go to everyone at McMaster Interfacial Technologies Group. Your friendship and selfless help makes me feel like in a big family and never feel lonely.

Finally, I wish to thank the laboratory manager Doug Keller, to office secretary Frances Lima, to graduate secretary Andrea Vickers, to Paul Gatt, James Lei, Justyna Derkach, Kathy Goodram, Lynn Falkiner and all the friends of Chemical Engineering for your assistance and help.

I like the life here and believe I will enjoy my continuing study life here for my PhD degree. Thanks, my friends!

Ruilin Li

Hamilton, Ontario

May 22nd 2008

Table of Contents

1 Introduction

In the textile industry, a large amount of dyes are released in the wastewater. The pollution of the industrially colored wastewater is very harmful for both the environment and human health. All wastewater need to follow the discharge standard (For dyes, it is 550 American Dye Manufacturers Institute (ADMI) units in Taiwan China[1] and 400 ADMI units in Korea[2]. It has been reported that some azo-dyes and their degradation products such as aromatic amines are highly carcinogenic[3, 4]. A safe, simple, low-cost and high-effective technology is needed to treat the colored wastewater.

1.1 Dyes and treatments

Among the textile dyes, azo type makes up 60-70% in the current market. It has been known that for azo dyes, the complexity of the structure determines the degree of stability[5, 6]. Reactive Black 5 (RB5) is one of the most difficultly removed reactive azo dyes due to its stability. The kinetics of the decomposition of RB5 is very important for the research of the dye degradation.

Dye removal technologies have been investigated to remove dyes by physical methods, chemical oxidative methods or biological methods. For the physical methods, adsorption and coagulation technologies can not decompose the dye structure and dye disposal is also a future pollution source. The traditional oxidative technologies, such as chlorination and ozonization, can degrade the dyes, but the by-products may be more harmful to human beings and the environment[7]. Chlorination can degrade dyes completely, but the chlorinated organics, which are formed in the process, are usually

more toxic than the dye itself. Ozone has no by-products in the process of oxidization. But the oxidizing power of ozone is too strong and the excess ozone may cause atmosphere pollution. The conventional biological methods are ineffective in most of dye degradation[6-8].

In contrast with the foregoing treatments, photocatalytic decomposition has many advantages. Photocatalytic decomposition is the process using semiconductors as catalysts to produce free radicals such as hydroxyl free radicals. The free radicals have strong oxidative power and can decompose organic dyes into small molecules such as CO_2, H_2O and inorganic anions[9, 10]. The excess free radicals cannot do harm to the human beings or the environment due to their short life[11, 12]. Now TiO_2 is widely used as a photocatalyst, because it is powerful, low-cost and environmentally friendly.

1.2 Literature review

1.2.1 Colloidal properties TiO_2

TiO_2 has three crystalline forms: rutile, anatase and brookite. In the research of photocatalysis, Degussa P25 (80% anatase and 20% rutile) is widely accepted as the standard[13, 14]. The primary particle size of the Degussa P25 is 21 nm and the specific surface area is 50±15 m^2/g.

The surface charge of TiO_2 is quite dependent on pH. It is known that the TiO_2 surface contains amphoteric titanol group (TiOH) which is controlled by the acid-base equilibria shown as Equation 1.1 and Equation 1.2[15]. For Degussa P25, pKa_1=4.5 and pKa_2 =8[16]. The isoelectric point of TiO_2 in aqueous suspension is 6.25[16] or 6[17]. Below the

isoelectric point, the surface of TiO_2 is positively charged. When the pH is much higher or much lower than the isoelectric point, the charged TiO_2 surface can adsorb oppositely charged species from the solution[18].

$$TiOH_2^+ \xleftrightarrow{pka_1} TiOH + H^+ \quad (1.1)$$

$$TiOH \xleftrightarrow{pka_2} TiO^- + H^+ \quad (1.2)$$

1.2.2 TiO_2 photocatalysis

TiO_2 is white powder because it has no light absorption at visible region. But it becomes reactive under the UV irradiation. Before 1970s, photo-bleaching by TiO_2 was reported in Japan[19]. It was also reported that some organic solvent, such as ethanol, could be oxidized under UV irradiation when TiO_2 was dispersed in it[19]. But the theory of TiO_2 photocatalysis was not developed in the academic field until Honda and Fujishima investigated it[20].

1.2.2.1 Mechanism of TiO_2 photocatalysis: Honda-Fujishima Effect

In 1972, Honda and Fujishima reported the electrochemical photolysis of water by TiO_2. They built an electrochemical cell which had a TiO_2 electrode and a platinum electrode (Figure 1.1[19]). When the TiO_2 electrode was irradiated under the <415 nm (3.0eV) light, oxygen was released from the TiO_2 electrode whereas hydrogen was released from the platinum electrode. They explained that when the energy of the photons

was greater than the band gap of TiO_2, the hole-electron (h^+-e^-) pairs were generated and separated (Equation 1.3). The holes (h^+) reacted with H_2O and formed oxygen at TiO_2 electrode (Equation 1.4) whereas the electrons (e^-) flowed to the platinum electrode and formed hydrogen at platinum electrode (Equation 1.5). They also measured the electrode potential to prove their theory[20]. This is well known as the first illumination of TiO_2 photocatalysis.

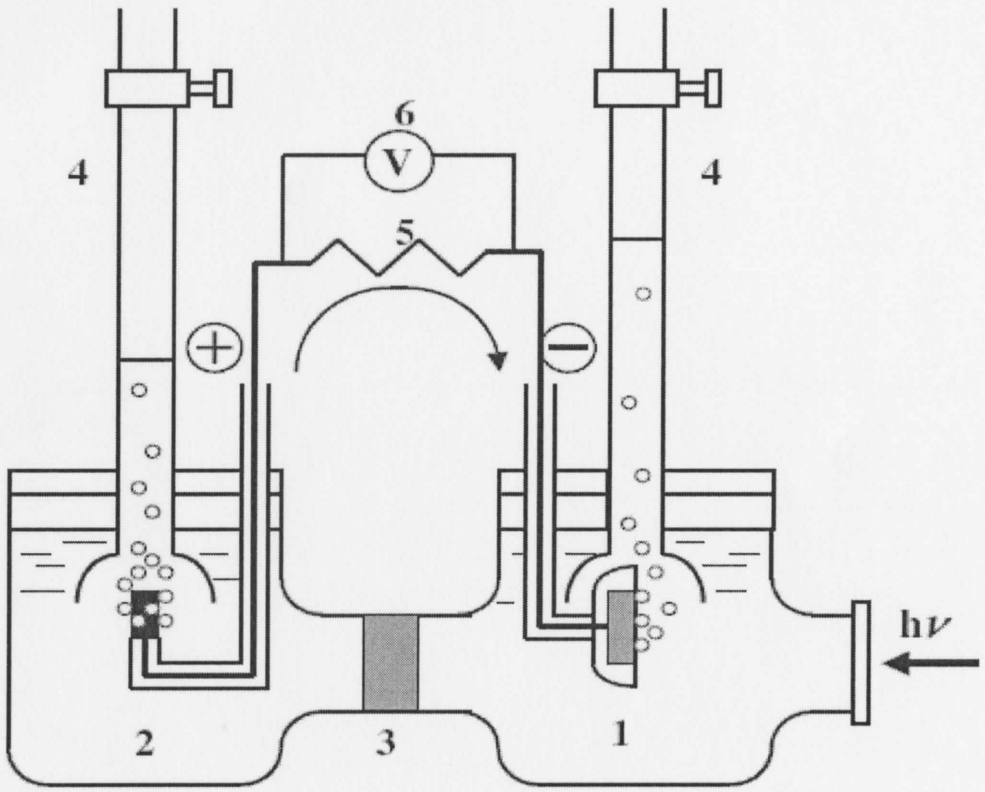

Figure 1.1 Schematic diagram of electrochemical photocell. (1) n-type TiO2 electrode; (2) platinum black counter electrode; (3) ionically conducting separator; (4) gas buret; (5) load resistance; and (6) voltmeter[19].

$$TiO_2 + 2\,hv \longrightarrow 2\,e^- + 2\,h^+ \quad (1.3)$$

$$2h^+ + H_2O \longrightarrow 1/2\,O_2 + 2\,H^+ \quad (1.4)$$

$$2\,e^- + 2\,H^+ \longrightarrow H_2 \quad (1.5)$$

$$H_2O + 2\,hv \longrightarrow 1/2\,O_2 + H_2 \quad (1.6)$$

1.2.2.2 Energy of the TiO_2 photocatalysis

Following Honda and Fijishima, Kawai and Sakata reported that the H_2 production by TiO_2 photocatalysis can be improved by 50% with the presence of ethanol. Most of organic molecules can improve the H_2 producing efficiency because the redox potential of the holes (h^+) is +2.53V versus standard hydrogen electrode. So the most organic compounds can be oxidized completely into small molecules such CO_2 and H_2O in theory[21].

Among the three types of TiO_2, anatase (E_G=3.2 eV) performs better than rutile (E_G=3.0 eV) for the TiO_2 photocatalytic decomposition. That is probably because anatase has the higher reduction potential of the photoelectrons (e^-)[22]. For the Degussa P25 the band gap is 3.2 eV.

1.2.2.3 Decomposition of organics

The application of TiO_2 powder for the decomposition of organic pollutants was firstly reported by Frank and Bard in 1977. They compared the decomposition of cyanide

in the presence of different types of TiO_2 aqueous suspension. The results proved the strong oxidative power of TiO_2 and also that anatase type TiO_2 had the strongest photocatalytic decomposition power[23]. After that, more and more researchers started the study on the TiO_2 photocatalytic decomposition of harmful compounds, especially on organic solvent and azo type dyes (Table 1.1).

Table 1.1 Organic solvents and dyes which can be decomposed by TiO_2 photocatalysis

Organic solvent or dyes	Year of publication	Reference
Cyanide	1977	23
Chloroform	1991	16
Acetaldehyde	1995	24
Basic Yellow 15 and Direct Blue 87	1995	25
Ethanol	1996	26
Merocyanine 540	1999	27
Toluene	1999	28
Remazol Black B and Remazol Turquoise Blue G 133	1999	29
Methylene blue	1999	30
Benzene and chlorobenzenes	2001	31
Sulforhodamine B, alizarin red and malachite green	2002	32
Acid Red 14	2003	33
azo-Methyl Red and Orange G	2003	4
Reactive Black 5 and Reactive Yellow 145	2005	3
Acetone	2008	34

1.2.2.4 Development of the mechanism of TiO_2 photocatalytic decomposition

Researchers have done a large body of research about TiO_2 photochemistry[15, 35]. Following the Honda-Fujishima mechanism, research also demonstrated that the photoelectrons (e^-) were generated in the conduction band and the holes (h^+) in the valence band (Equation 1.7) at the surface of TiO_2 which was irradiated by the UV light (wavelength < 380nm)[36-38]. The holes could react with water or hydroxyl anions to generate hydroxyl free radicals (Equation 1.8 and 1.9) which had high reactivity to break the organic structure and oxidize organic molecules into small molecules such as CO_2 (carbon dioxide) and H_2O (water). In addition, some strong-oxidative forms of active oxygen, such as O_2^-, ·OH, HO_2· and O· were also generated in the process of TiO_2 photocatalysis (Equation 1.9-1.12) and might decompose the harmful compounds[39, 40].

$$TiO_2 + hv \longrightarrow TiO_2 (e^-, h^+) \quad (1.7)$$

$$h^+ + H_2O \longrightarrow \cdot OH + H^+ \quad (1.8)$$

$$h^+ + OH^- \longrightarrow \cdot OH \quad (1.9)$$

$$e^- + O_2 \longrightarrow O_2^- \quad (1.10)$$

$$O_2^- + H^+ \longrightarrow HO_2 \cdot \quad (1.11)$$

$$h^+ + O_2^- \longrightarrow 2O \cdot \quad (1.12)$$

It has been concluded that organic molecules may have two ways to be decomposed by TiO_2 photocatalysis (Figure1.2[41]). One is to be oxidized directly by the hole (h^+) at the valence band [17, 41, 42]. The other is to be oxidized by the free radicals.

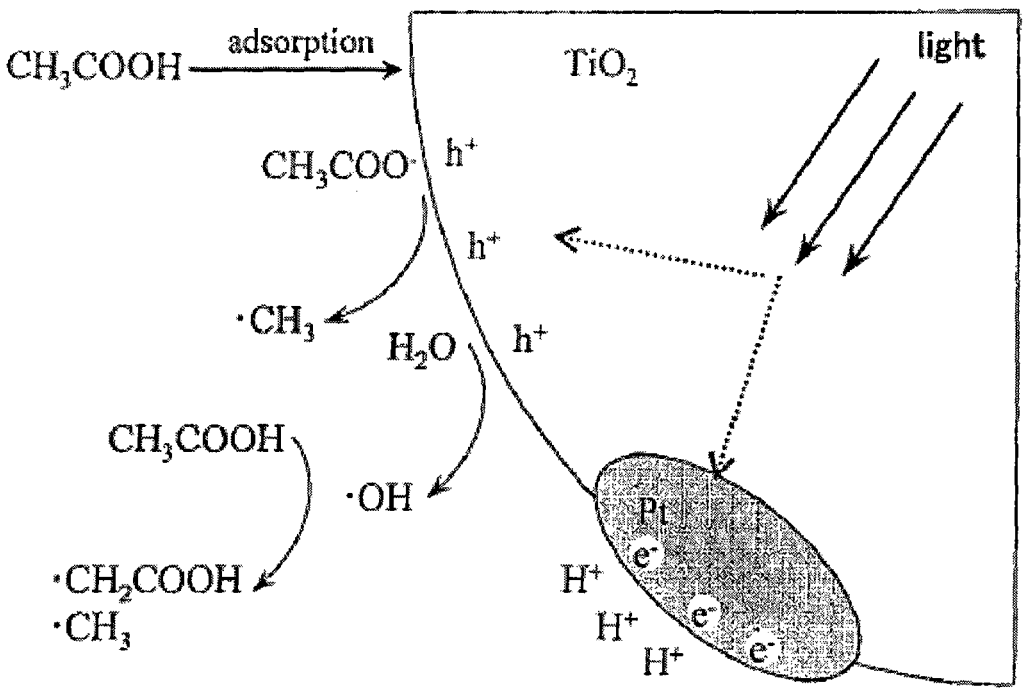

Figure 1.2 Adsorbed organics can be directly oxidized by the hole (h+) or can be oxidized by the free radicals[41].

1.2.2.5 Effect of O_2 and H_2O_2

The rate of the TiO_2 photocatalytic decomposition of organic compounds can be significantly improved in the presence of oxygen. The recombination of the electrons (e^-) and holes (h^+) is believed to reduce the efficiency of photocatalytic decomposition. Oxygen, which works as the electrons (e^-) adopter, might block the recombination by a

series of reactions (Equation 1.9-1.12)[15, 17, 43]. The generated superoxide, such as O_2^-, can also attack organic molecules which are adsorbed at TiO_2 surface[17, 44]. Both the reduction of the hole-electron pair recombination and the generation of superoxide result in the improvement of photocatalytic decomposition.

Hydrogen peroxide (H_2O_2) may also contribute to the TiO_2 photocatalytic decomposition. Lots of researchers reported that adding H_2O_2 can improve the rate of photocatalytic decomposition[45-47]. H_2O_2 is one type of electron adapter which may reduce the hole-electron pair recombination[47]. Also H_2O_2 can improve the chance of free radicals reacting with organics in solution. Some researchers reported that the bacteria 50-70μm away from TiO_2 surface could also be killed by TiO_2 photocatalysis[48]. They also captured some reactive oxygen species, such as H_2O_2 which was produced by free radicals (Equation 1.13), at the place 50-70μm away from TiO_2 surface. They explained it that the reactive oxygen species diffused and killed the bacteria due to their strong-oxidative power. Also the H_2O_2 could be separated into two free radicals again[48] (Equation 1.14).

$$\cdot OH + \cdot OH \longrightarrow H_2O_2 \qquad (1.13)$$

$$H_2O_2 \xrightarrow{\text{UV or heat}} \cdot OH + \cdot OH \qquad (1.14)$$

1.2.2.6 TiO_2 film

From 1990, people began doing research on TiO_2 film, but not on TiO_2 suspension, for two reasons. The first is the nature of TiO_2. TiO_2 is white powder which

can block the UV light. So the UV light can not transmit through the TiO_2 suspension. The second is that the power of UV from the sunlight is only several hundred $\mu W/cm^2$ and it can only support limited TiO_2 photocatalysis[19].

Many groups have developed photocatalytic films by coating TiO_2 on paper, nonwoven fabrics and glass. In 1995, Matsubara and his coworkers reported the first TiO_2-containning paper. They found that the TiO_2 coated paper had better photocatalytic efficiency than Degussa P25[49]. After this observation, more and more types of TiO_2 film were made to get better effect of TiO_2 photocatalytic decomposition. Table 1.2 shows some TiO_2 film samples and their fabrications.

Table 1.2 Types of TiO_2 film and their fabrications.

Type of TiO_2 film	Fabrication	Year of publication	Reference
Transparent TiO_2 film	Self-assembly	2008	50
TiO_2 coated paper	Wet-end addition	2003	51
TiO_2 coated paper	Size press treatment	2004	52
TiO_2 coated glass	Spin coating	1999	53
TiO_2 film	Dip coating and blade deposition	2002	54
TiO_2 coated glass	Sol-gel spin coating	2008	55

1.2.3 Kinetics of theTiO_2 photocatalytic decomposition

1.2.3.1 Langmuir-Hinshelwood model

Langmuir-Hinshelwood (LH) model has been widely accepted for the kinetics of TiO_2 photocatalytic decomposition[56-59]. LH model is derived from the Langmuir model which indicates the adsorption at a solid – liquid interface. It assumes that (1) the number of the sites for the adsorption is fixed; (2) only one molecule can be adsorbed at one site; (3) every site is filled with either solute molecule or solvent molecule; (4) the adsorption is at the equilibrium state and the rate of the adsorption is much larger than other chemical reactions; (5) no reactions between the molecules adsorbed at the surface. So from the Langmuir model, the moles of the adsorbed solute molecules n_2^s can be written as

$$\frac{1}{n_2^s} = \frac{1}{n^s \bullet b \bullet C_{eq}} + \frac{1}{n^s} \qquad (1.15)$$

or

$$\frac{n_2^s}{n^s} = \frac{bC_{eq}}{1 + bC_{eq}} \qquad (1.16)$$

Where n_2^s is the moles of the solute adsorbed at TiO_2 surface (Unit: $mol \cdot kg^{-1}$); n^s is the moles of the sites which can adsorb molecules at TiO_2 surface (Unit: $mol \cdot kg^{-1}$); b equals K/a_1, where $K=N_2^s a_1 / N_1^s a_2$, $N_1^s$and N_2^s are the mole fraction of solvent and solute adsorbed at TiO_2 surface when the adsorption is at equilibrium state, a_1 and a_2 are the activities of solvent and solute (Unit: $m^3 \cdot mol^{-1}$); C_{eq} is the concentration of the solute in the bulk at the equilibrium state (Unit: $mol \cdot m^{-3}$).

The kinetic rate can be written as

$$r_{LH} = \frac{dC}{dt} = k(\frac{bC_{eq}}{1+bC_{eq}}) \quad (1.17)$$

or

$$\frac{1}{r_{LH}} = \frac{1}{k \bullet b \bullet C_{eq}} + \frac{1}{k} \quad (1.18)$$

The linearity of a plot of a $1/r_{LH}$ versus $1/C_{eq}$ has been proved by lots of experiments. The parameters can be also obtained by the slope 1/kb and the y intercept 1/k.

1.2.3.2 Serial steps reaction model

It is reported that photocatalytic dye degradation is a first-order reaction in the concentration of the dye[60-62]. Tanaka and his coworkers measured the photocatalytic degradation of 7 dyes and concluded that the photocatalytic degradation should be first-order and the rate constant was from 0.007 min^{-1} to 0.032 min^{-1} [61]. The single-step first-order model (Equation 1.20) was concluded from those experiments. The change of the dye concentration (C_D) is just a function of the first-order rate constant (k) and time (t) which is written as

$$r = \frac{dC_D}{dt} = -kC_D \Rightarrow C_D = C_D(0)\exp(-kt) \quad (1.19)$$

where r is the decomposition rate and $C_D(0)$ is the initial concentration of the dye.

$$\text{dye} \xrightarrow{k} \text{products} \qquad (1.20)$$

Julson and his coworkers reported that the data of the semilog plot of the absorbance was not linear in time. They found that the semilog plot had two regions and suggested a two-step first-order model which had an intermediate state before the dye was completely decomposed (Equation 1.23)[63]. The model can be described as

$$\frac{dC_D}{dt} = -k_1 C_D \Rightarrow C_D = C_D(0)\exp(-k_1 t) \qquad (1.21)$$

and

$$\frac{dC_I}{dt} = k_1 C_D - k_2 C_I \Rightarrow C_I = \left(\frac{k_1 C_D(0)}{k_2 - k_1}\right)(\exp(-k_1 t) - \exp(-k_2 t)) \qquad (1.22)$$

where C_I is the concentration of intermediate products; k_1 and k_2 are first-order reaction rate constants.

$$\text{dye} \xrightarrow{k_1} \text{intermediate} \xrightarrow{k_2} \text{final products} \qquad (1.23)$$

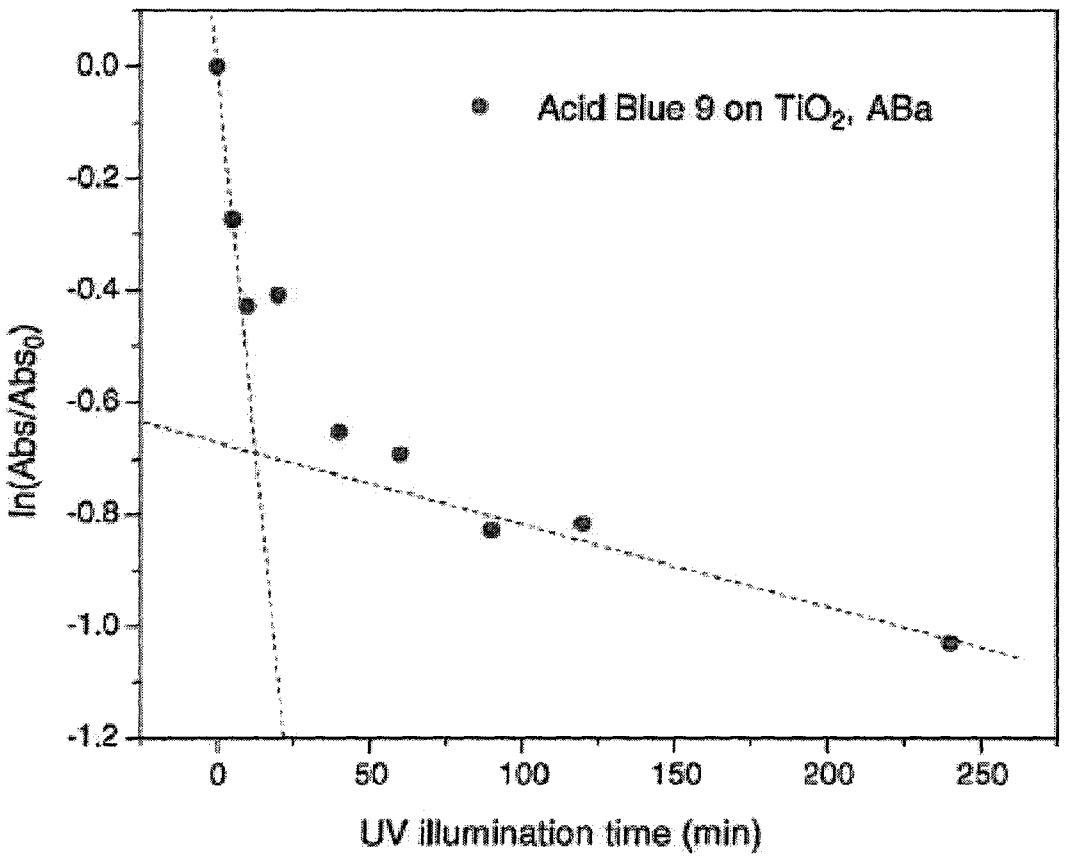

Figure 1.3 ***Julson showed the photocatalytic decomposition data which not fit the single step model[63].***

They used the absorbance (Abs) instead of the concentration (Beer-Lambert Law Abs=abC) and gave the final expression as

$$Abs(t) = Abs(0)((\frac{\alpha_I}{\alpha_D}\frac{k_1}{k_2 - k_1})(\exp(-k_1 t) - \exp(-k_2 t)) + \exp(-k_1 t)) \quad (1.24)$$

where α_D and α_I are the molar absorptivities of dye and intermediate products. The two-step first-order model is quite fit for the photocatalytic decomposition data of RB5 (SD<5%).

1.2.3.3 UV intensity dependent model

Many researchers have reported that the UV intensity can influence the photocatalytic decomposition of organics[64-66]. It was also reported that the rate of the isopropanol decomposition by TiO_2 photocatalysis was proportional to the UV intensity[67, 68]. Julson et. al. supposed a UV intensity influenced model from the former work. It assumed that only the TiO_2, which was directly illuminated by UV light, could decompose organic dyes (Figure 1.4[63]) and the rate constant k was a function of UV intensity which was determined by the effective absorption coefficient of TiO_2 (α_T), the intensity exponent (a) and the axial coordinate through the TiO_2 layer (y) (Figure 1.5[63]). The concentration at y from a position of the TiO_2 surface with t time illumination ($C_D(y,t)$) can be described as

$$\frac{dC_D}{dt} = -k_0 \exp(-\alpha_T a y) C_D(y,t) \tag{1.25}$$

$$\Rightarrow C_D(y,t) = C_D(0) \exp(-k_0 t \exp(-\alpha_T a y)) \tag{1.26}$$

and the average concentration of the dye ($\overline{C_D}(t)$) can be described as

$$\overline{C_D}(t) = \frac{1}{L} \int_0^L C_D(0) \exp(-k_0 t \exp(-\alpha_T a y)) dy \tag{1.27}$$

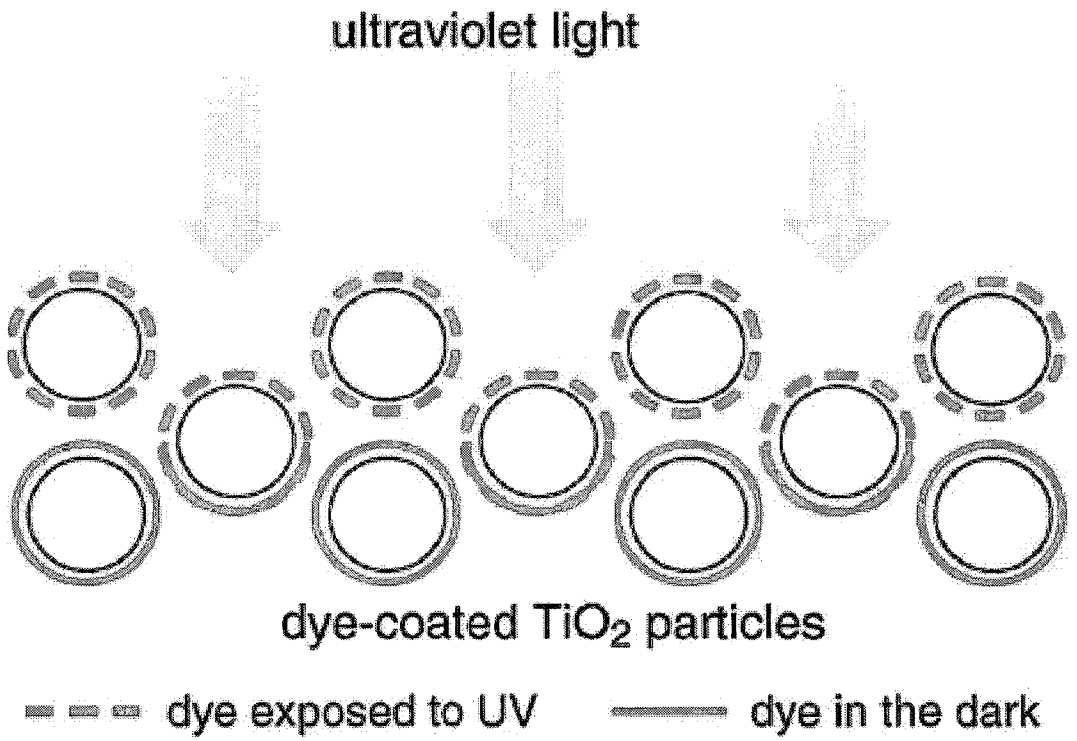

Figure 1.4 The dyes can only be decomposed by the directly illumined TiO_2[63].

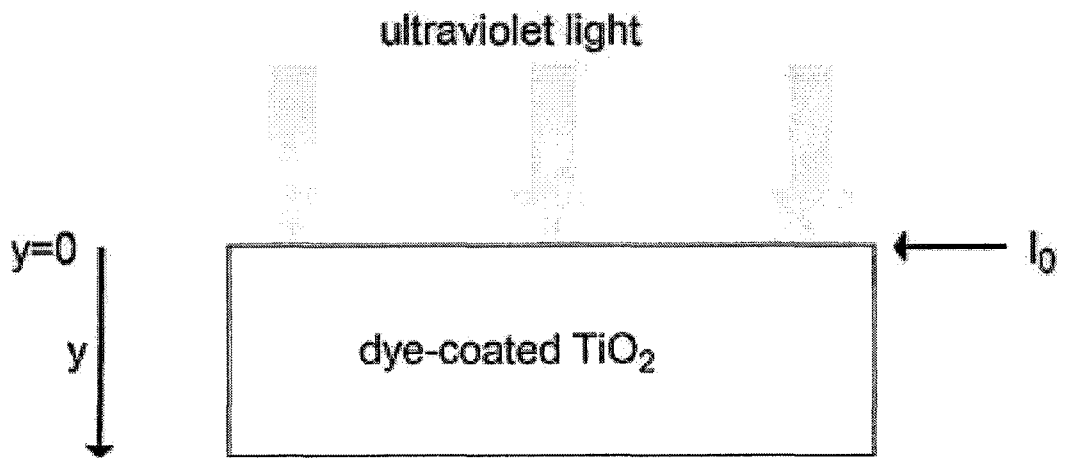

Figure 1.5 UV intensity dependent model[63].

1.3 Objective

The purpose of this project was to develop a new kinetic model for the decomposition process of the organic dye Reactive Black 5 (RB5). The effects of pH, ionic strength and the temperature of the dye solution, as well as the UV intensity of the light source, the solution flow rate and the amount of TiO_2 deposited on the paper were studied to find their correlation with the decomposition rate.

1.4 Thesis outline

In this work, the effect of TiO_2 coated paper for dye decomposition is studied at different conditions. Background knowledge and literatures published on this purpose is reviewed in Chapter One. Experiments and characterizations are in Chapter Two, all the experimental results are in Chapter Three, and discussion of results is in Chapter Four. A kinetics model is built for better understanding TiO_2 photocatalytic decomposition in Chapter Five. The conclusions are shown in Chapter Six.

2 Experimental

2.1 Materials

Titanium Dioxide (TiO_2 P25, Aeroxide, Degussa) was used as the photocatalyst. TiO_2 P25 contains 80% anatase and 20% rutile. The specific surface area of TiO_2 P25 particles is 55 ± 15 m^2/g and the average primary particle size is 21 nm. The pH of the 4% TiO_2 P25 dispersion is around 3.4 - 4.5. Reactive Black 5 (RB5, 55%, Aldrich) was used as the organic dye sample. The molecular structure is shown in Figure 2.1. It contains 4 electrons per molecule in the aqueous solution according to its structure. Filter Papers (Whatman® Type 4, d=15 cm) were used for preparing TiO_2 coated paper. They are made from cellulose. The particle retention is 20 - 25 μm, which is good at filtering coarse particles and gelatinous precipitates. AMBERJET® 1200 (H) ion exchange resin (Rohm & Haas) was used for desalting of the intermediate products. All other chemicals and solvents were used as purchased.

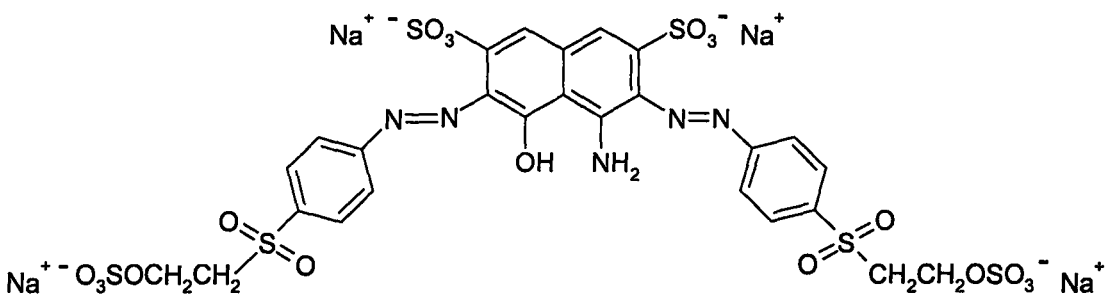

Figure 2.1 The molecular structure of RB5.

2.2 Characterization of TiO_2 particle

The electrophoretic mobility of the TiO_2 suspension was measured in a square cuvette (BIC BI-SCP cuvette, 10mm square, 4 ml capacity) by BIC Zeta Plus Zeta Potential Analyzer (Holtsville, NY) with a 26 mW laser. The software is palsw32 version 3.54. The TiO_2 suspension was prepared in 5×10^{-3} M NaCl solution at the required pH before measurement. The electrophoretic mobility of TiO_2 in 3.5×10^{-3} mM RB5 solution was also measured with 5×10^{-3} M NaCl added into the RB5 solution. The standard deviation of 6 measurements was used to estimate the error bars.

The particle size distribution of TiO_2 P25 was measured using the MALVERN Mastersizer 2000. The software is Mastersizer 5.1. 1.0 mg/mL TiO_2 suspension was prepared in a 20 mL vial before measurement. 500 mL water was injected into the accessory Hydro 2000. Ultrasonic and stirring was opened to disperse TiO_2 suspension. The TiO_2 suspension was injected into Hydro 2000 drop by drop until the signal reached measurable scale. The data was recorded by the computer.

2.3 Preparation of TiO_2 coated paper

A paint sprayer (Wagner Power Painter PRO, 2400 PSI) was used to coat TiO_2 on the surface of the filter paper. Before being sprayed, the filter paper was placed on a steel plate (Φ=16cm), which was supported by a plastic ring. The sprayer was fixed 10cm above the filter paper by clamps and stands. The prepared TiO_2 suspension was sprayed for 5 seconds for each sheet of the filter paper. The wet TiO_2 coated paper was dried in

air in a controlled room where the temperature was 23.0±0.2°C and the humidity was 50±1%. Figure 2.2 shows the apparatus used in preparing the TiO_2 coated paper.

Figure 2.2 The TiO_2 coated paper preparing apparatus.

2.4 Characterization of the TiO_2 coated paper

The amount of TiO_2 coated on the filter paper is determined from the difference between the mass of the filter paper and the mass of TiO_2 coated paper. Both of the paper samples were dried in an oven at 105°C for 3 hours before measuring the mass. Table 2.1 shows the TiO_2 content for different TiO_2 coated paper samples. Paper sample name is

defined as TOP (TiO_2 on top) plus the concentration of the TiO_2 suspension sprayed (mg/ml).

Table 2.1 Classification of paper samples

Paper Sample Name	The concentration of TiO_2 suspension sprayed / $mg \cdot ml^{-1}$	TiO_2 content / $mg \cdot cm^{-2}$
TOP0	0	0
TOP0.2	0.2	Not measured
TOP5	5	0.51±0.09
TOP10	10	0.98±0.09
TOP20	20	1.56±0.10

2.5 Measurement of the dye decomposition

A continuous flow apparatus was built for measuring the dye concentration in the decomposition experiments (Figure 2.3). The reactor was a glass tube (40mm length, d=10mm) with the light source provided by a UV bench lamp (367nm, 15W, XX-15BLB Black-Ray®, Entela) in a UV protection chamber. The absorbance of the dye solution was measured in a UV flow cell (pathlength=10mm, Beckman) by DU® 800 spectrophotometer (Beckman-Coulter). The temperature of the dye solution was measured by a digital thermometer (±0.5°C, Fisher Scientific), whose sensor was inserted into the tubular reactor, and pH was measured by pH Meter 140 (Corning). Plastic tubes (1/32 inch ID × 1/32 inch wall, Tygon Saint Gobain) were used to connect all the instruments. The whole system could hold 10ml of dye solution.

Before the measurement, the dye solution was prepared in a 20ml vial. 1M standard HCl solution and 1M standard NaOH solution were used to alter the sample pH from 2 to 7. For changing ionic strength, 1 M NaCl solution was added into the samples. A water bath was used to control the sample temperature. Different UV intensities were obtained by adjusting the distance between the UV lamp and the glass tube. The flow rate of dye solution was altered by controlling the pump speed.

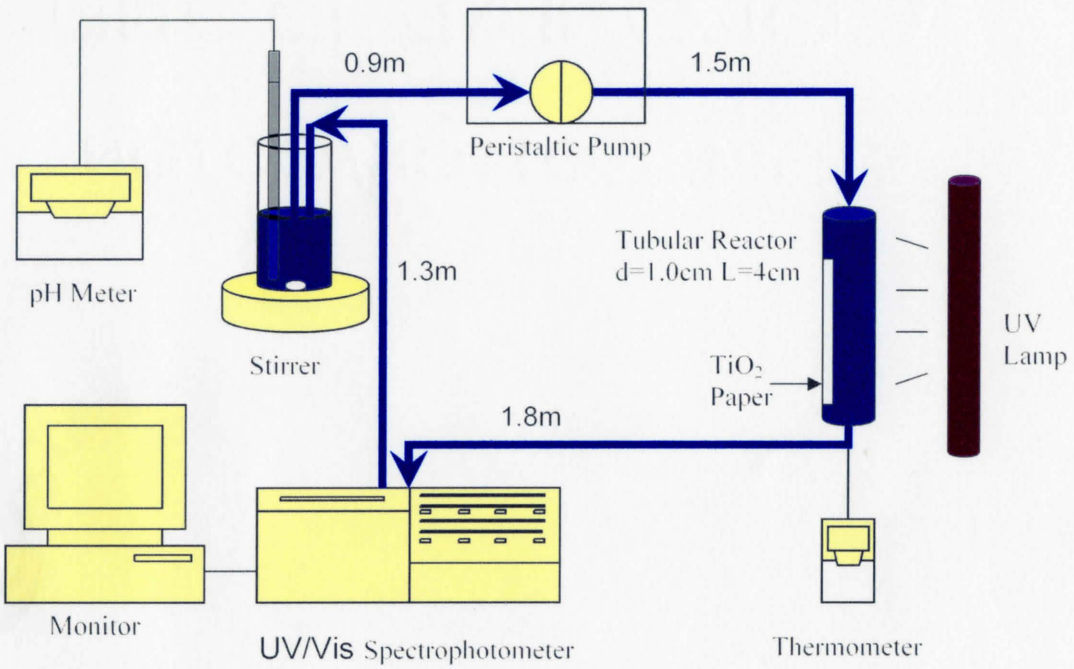

Figure 2.3 The decomposition measuring apparatus.

When decomposition measurement started, one piece of TiO_2 coated paper (1.0×3.0cm) was placed into the tubular reactor. A speed-controllable peristaltic pump (Std. Console, 100rpm, MasterFlex) was used to circulate the dye solution in the whole

system. Before turning on the UV lamp, the dye solution was circulated for 10 minutes to make sure the adsorption of dye at TiO_2 surface was at equilibrium state. The absorbance of the dye solution was recorded every 6 seconds by the spectrophotometer after the decomposition was started. The concentration of the RB5 solution was determined by the absorbance at 597 nm (Figure 2.4) and the concentration of the intermediate products was determined by the absorbance at 521 nm (Figure 2.5).

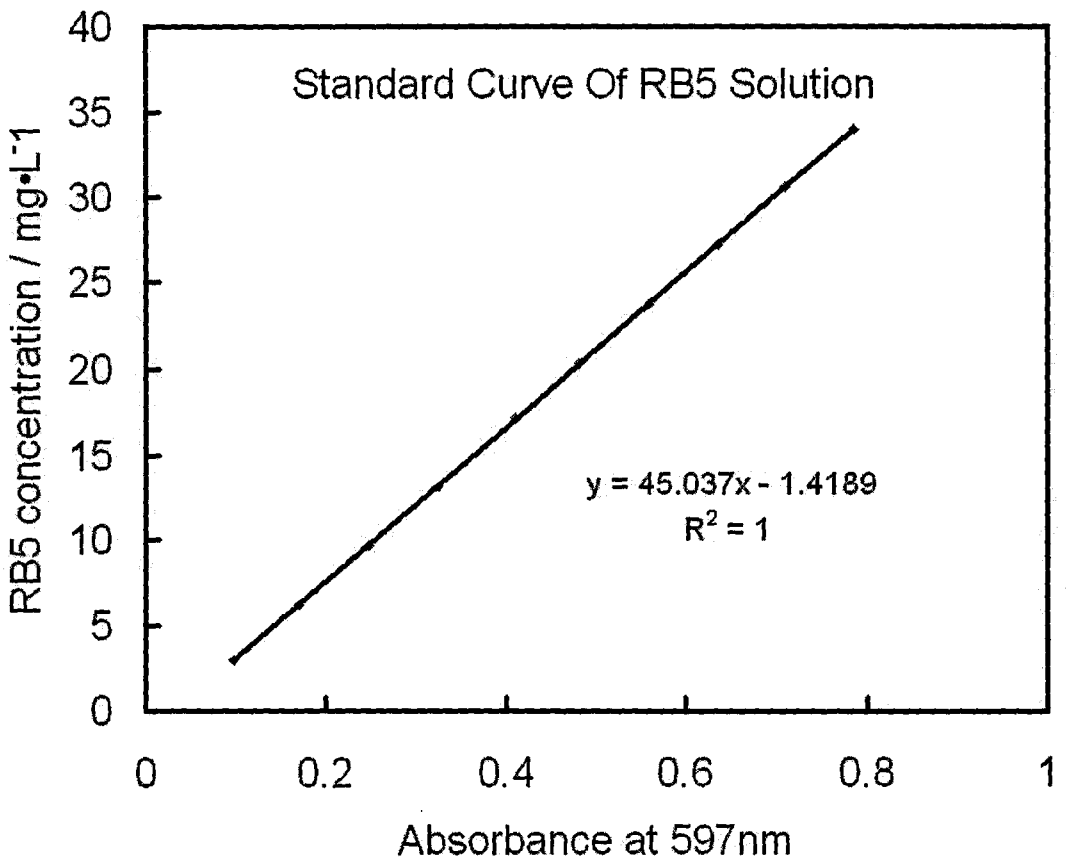

Figure 2.4 Absorbance at 597nm vs. the concentration of the RB5 solution

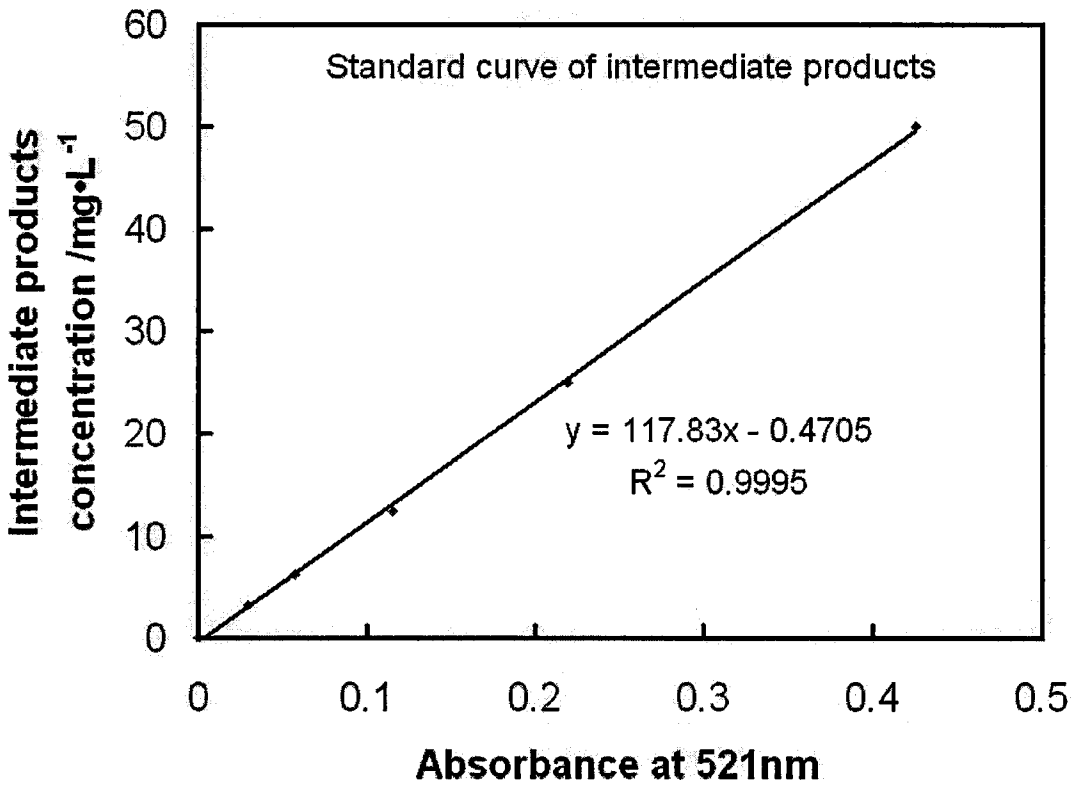

Figure 2.5 ***Absorbance at 521nm vs. the concentration of the intermediate products solution***

Residence time distribution (RTD) of the apparatus was also measured. 9 mL water was added into the apparatus at the beginning. When the measurement started, 1mL of 35 mg/L RB5 solution was injected into the tubing just at the pump. The concentration of RB5 solution, which flowed through the spectrophotometer at different time, was recorded automatically by the computer.

2.6 Detection of the desorption of TiO_2 from paper surface

When TiO_2 particles are released from paper to the solution, the absorbance of the original solution should increase because the TiO_2 particle can block the transmitted light. So measuring the absorbance of the solution can detect the desorption of TiO_2. The desorption of TiO_2 from the paper surface was detected using the same apparatus as shown in Figure 2.3. The TiO_2 coated paper sample (1.0×3.0cm) was placed into the tubular reactor without UV irradiation. The system was run and the data were recorded the same way as during the decomposition experiment.

2.7 Measurement of UV intensity in the glass tube

The UV intensity of the UV lamp was measured by a Traceable® Ultra Violet Light Meter (Figure 2.6). Before the measurement, the glass tubing reactor was cut into two half-circled parts. The sensor of the light meter was covered by the half-circled glass tubing parts. Therefore, the exact UV intensity in the glass tube reactor can be obtained. Table 2.2 shows the data of the UV intensity with the distance between the UV lamp and the glass tube.

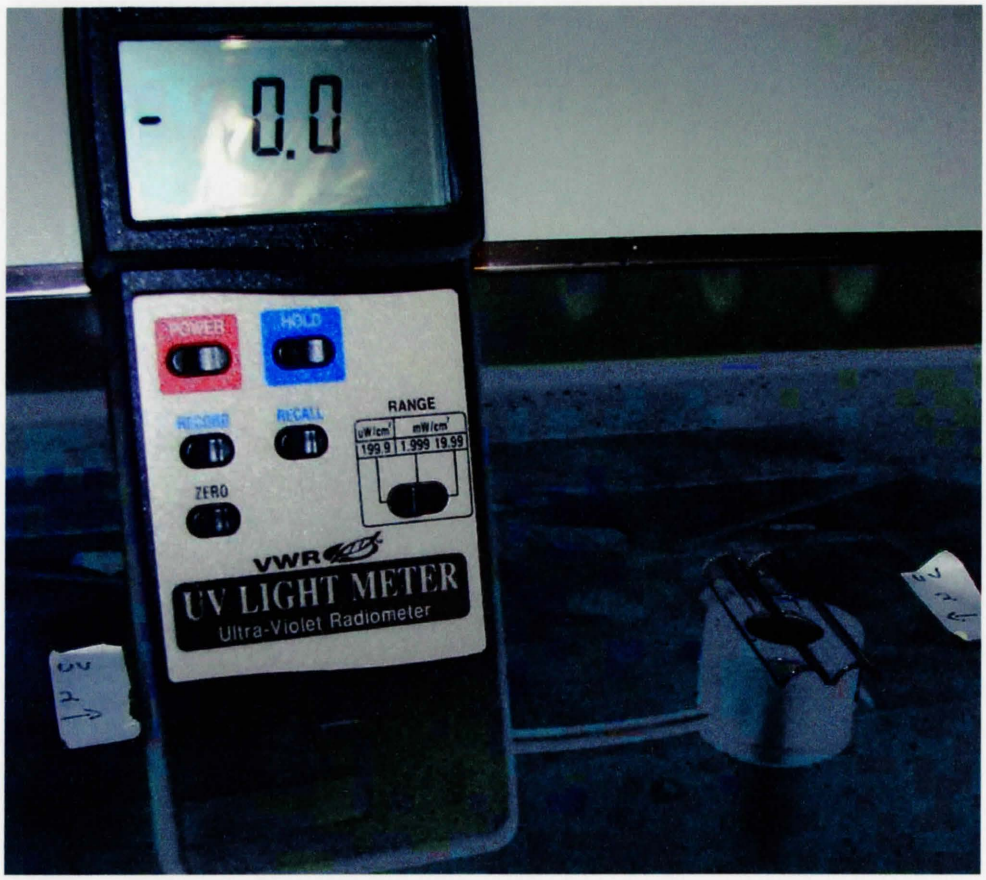

Figure 2.6 Measurement of UV intensity in the glass tube.

Table 2.2 UV intensity table

	Distance between the UV lamp and the glass tube / cm	UV intensity / $mW \cdot cm^{-2}$
1	6	1.02±0.01
2	8	1.15±0.01
3	10	1.28±0.01
4	12	1.39±0.01
5	14	1.58±0.01
6	16	1.70±0.02
7	18	1.87±0.01

2.8 Measurement of dye adsorption on TiO_2

Dye samples of different concentration were prepared before the adsorption measurement. 10 ml dye solution sample and 10 mg TiO_2 were added in a 20 ml glass vial and were kept in dark for 1 hour before the sample was centrifuged at 16000 rpm for 10 minutes (Centrifuge 5415D, Eppendorf). The absorbance of the solution layer was measured to calculate the concentration. The dye adsorption was determined as the difference between the initial concentration of the dye solution and the final concentration of the upper solution.

2.9 Intermediate products and desalting of the intermediate products

The intermediate products were obtained by decomposing the RB5 solution in 1M NaCl. To get the pure intermediate products, desalting was necessary. Firstly, the intermediate product solution was concentrated into a saturated solution at 50°C by a rotary evaporator (Rotavapor R-200, BÜCHI). Then ethanol (95%) was added into the saturated solution at 1:1 volume ratio, and NaCl crystals were separated out by filtering. The steps were repeated until the total volume of the intermediate products solution was around 10 ml. The 10 ml intermediate products solution was then diluted to 200 ml again and passed through the column filled with ion exchange resin to make sure all the Na^+ being removed. The filtrate was freeze dried and named as the "no salt" sample.

3 Results

3.1 Properties of the TiO_2 coated paper

3.1.1 Adsorption of TiO_2 on filter paper

3.1.1.1 Properties of TiO_2 particles

Some important properties of TiO_2 particles, such as the particle size and the property and density of surface charge, can determine the stability of TiO_2 at the paper surface. The decomposition rate of the TiO_2 coated paper is also dependent on the TiO_2 properties.

The electrophoretic mobility was measured from pH 2 to pH 9 to determine the surface charge of TiO_2. From the electrophoretic mobility measurement (Figure 3.1), the zero charge point of TiO_2 P25 is around pH 5. The surface charge of TiO_2 P25 is negative at pH > 5 and positive at pH < 5. So pH is the key in controlling TiO_2 surface charge, which is very important for the adsorption of TiO_2 on the oppositely charged surfaces[69].

The particle size distribution of the TiO_2 suspension was measured by Mastersizer 2000. Figure 3.2 shows the particle size distribution of TiO_2 P25 in the aqueous suspension. The average size of TiO_2 P25 in aqueous suspension is 0.242 μm (surface weighted mean) and the span of the particle size ($\frac{D_{90}-D_{10}}{D_{50}}$) is 2.53. The average surface area is around $5m^2/g$ from calculation. The particle size of TiO_2 in the aqueous suspension is bigger than 100 nm, the size of dry TiO_2 P25[36].

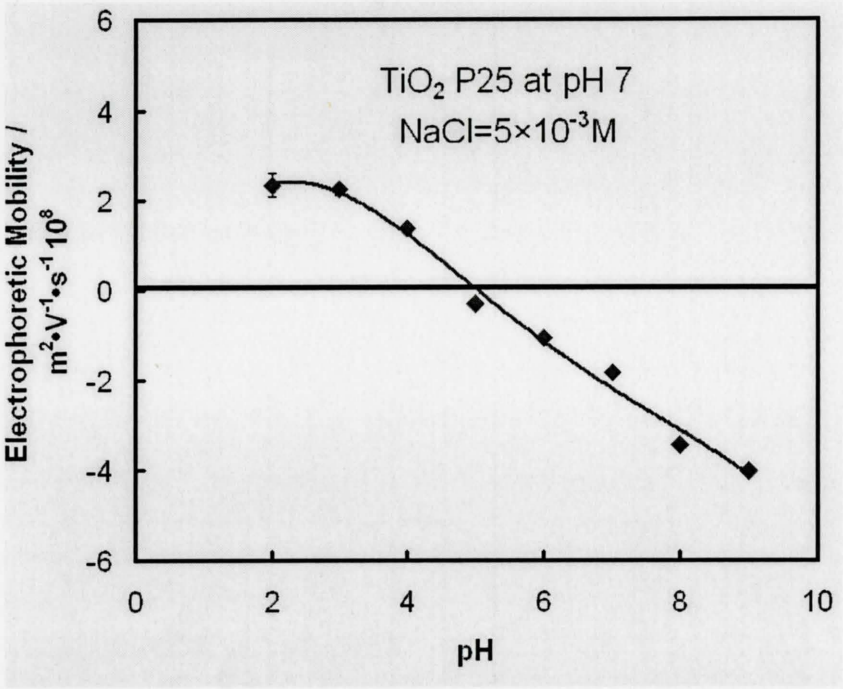

Figure 3.1 Electrophoretic mobility of the TiO2 suspension. ([NaCl]=5×10^{-3}M)

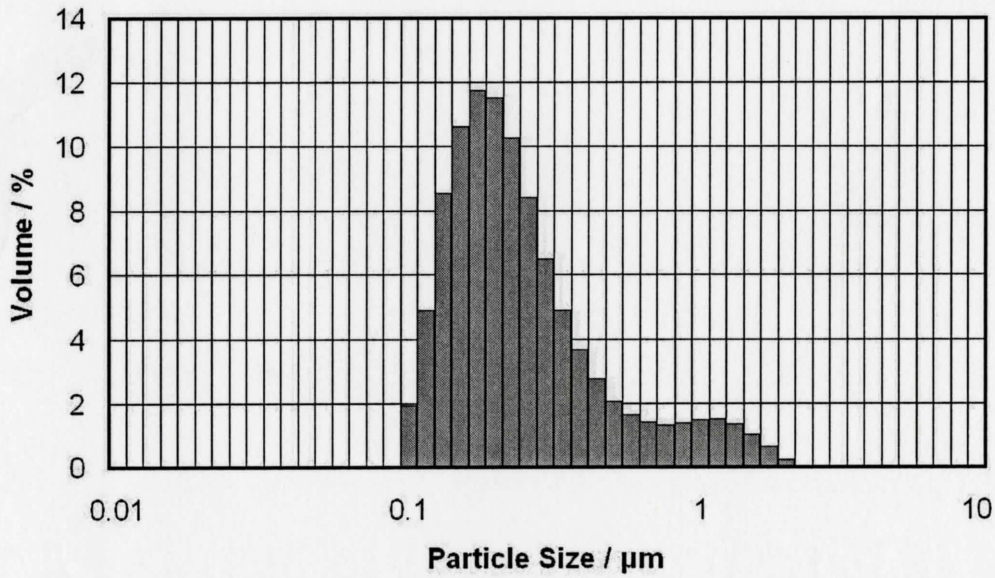

Figure 3.2 Particle size distribution of TiO_2 P25 in the suspension (pH 6.0, RT, stirring and ultrasonic dispersed).

3.1.1.2 Desorption of TiO_2 from paper surface

The desorption of TiO_2 from the paper surface was detected to make sure no TiO_2 particles were released in the decomposition experiments. Released TiO_2 would affect the measurement of the absorbance because TiO_2 particles could block or scatter light. The desorption of TiO_2 was detected in the RB5 solution from pH 2 to pH 10. Figure 3.3 shows the results of the desorption experiment at pH 7 and pH 10. For the blank sample at pH 7, no significant changes were found, which means no TiO_2 released from the paper surface. For the sample at pH 10, the absorbance increased by about 0.15, and that indicated TiO_2 was released from the paper surface. The results of the desorption measurements indicate that TiO_2 is released from the paper surface when pH $\geq$ 8 and isn't when pH $\leq$ 7.

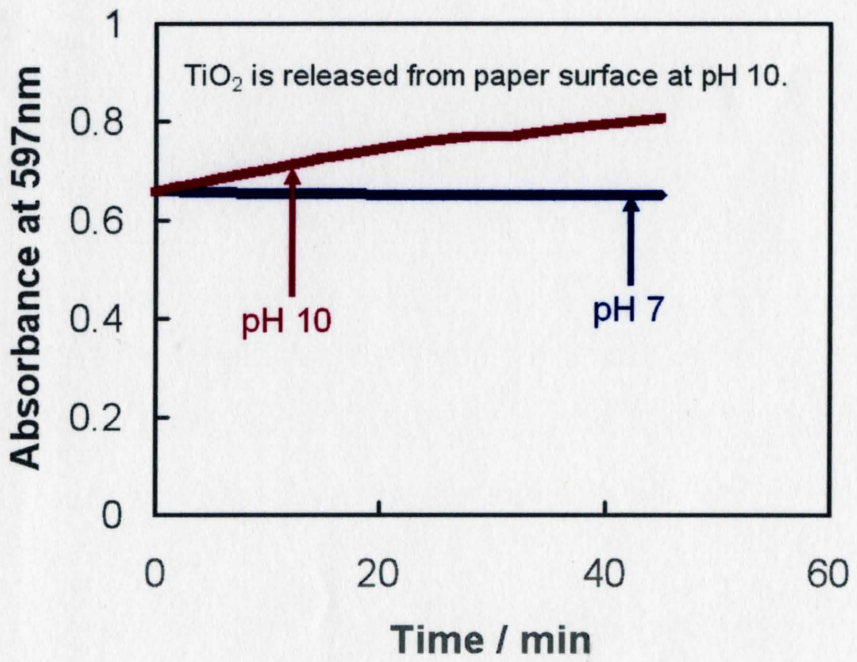

Figure 3.3 Results of the desorption experiments at pH 7 and at pH 10.

3.1.1.3 The surface structure of TiO_2 particles adsorbed on filter paper

Scanning electron microscopy (SEM) was used to examine the surface structure of TiO_2 coated paper. Figure 3.4 shows the SEM image of the surface structure of TiO_2 coated paper TOP0.2. It is found that only small amount of TiO_2 particles was imbedded into the fiber net or on the surface of fibers. The surface structure of TOP0.2 was similar to untreated filter paper. Figure 3.5 shows the SEM image of the surface structure of TiO_2 coated paper TOP5. The TiO_2 layer could be found covering the whole filter paper surface. In comparison with the complex surface structure of TOP0.2, TOP5 has a TiO_2 plate-like surface structure that was much easier to study. TOP10 and TOP20 have the same surface structure like TOP5. So TOP5, TOP10 and TOP20 were chosen as the samples in all related experiments.

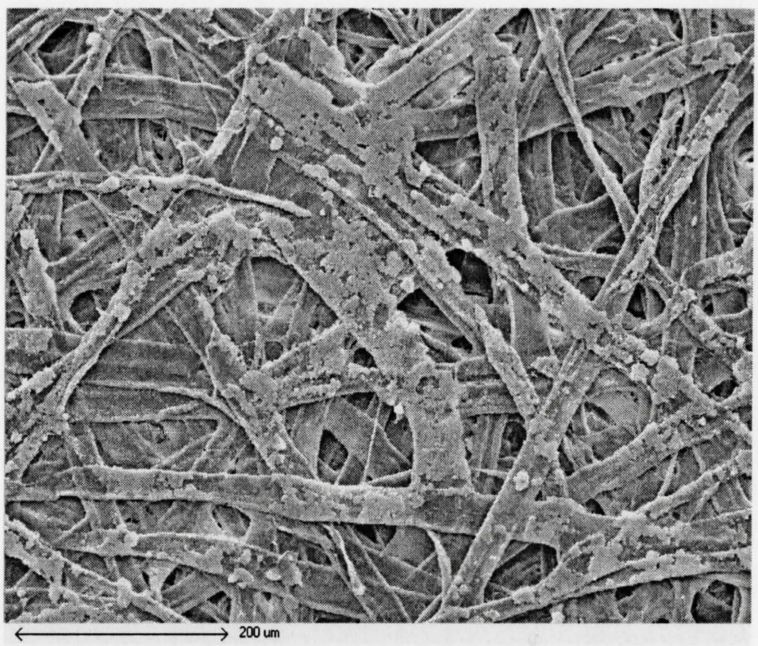

Figure 3.4 SEM image: surface of TOP0.2. (White powder is TiO_2)

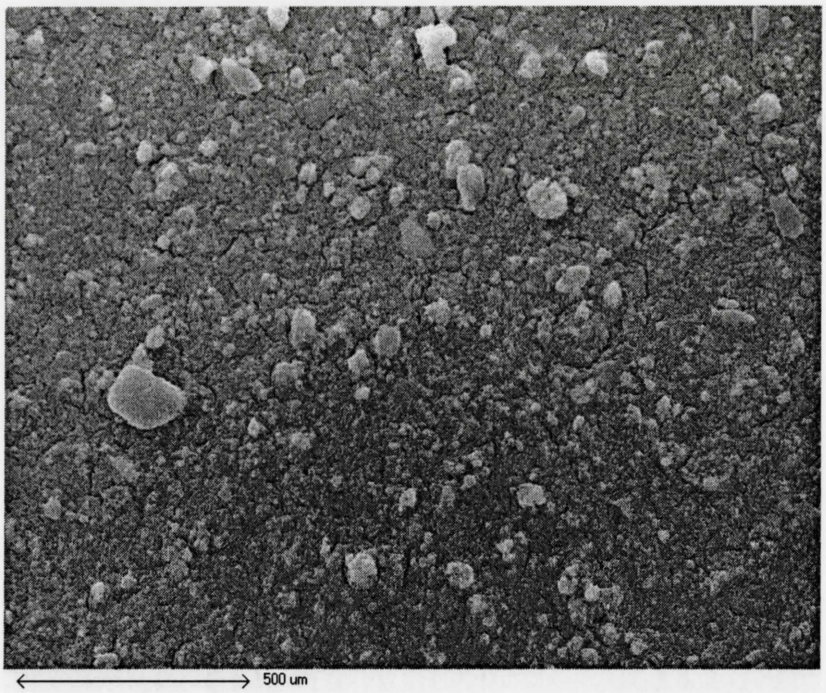

Figure 3.5 SEM image: surface of TOP5

3.1.2 Properties of RB5

3.1.2.1 Diffusion of RB5 in the measuring apparatus

The diffusivity of RB5 in water (D_{RB5}) was estimated by Polson correlation:

$$D_{RB5} = \frac{9.94\times10^{-15}T}{\mu M_A^{1/3}} = 2.97\times10^{-10} m^2/s \quad (3.1)$$

Where T is the absolute temperature (room temperature is 298K); μ is viscosity of the liquid medium (for water at 25°C it is 0.001 kg/m·s); M_A is the molecular weight of the solute (for RB5, it is 991.82 Da). From Fick's first law, the flux of RB5 from the solution to the paper surface (J_{RB5}) can be written as

$$J_{RB5} = -D_{RB5}\frac{dC_{RB5}}{dx} = 8.91\times10^{-6} kg/m^2 \bullet s \qquad (3.2)$$

where C_{RB5} is the concentration of RB5 solution (it is 3×10^{-3} kg·m^{-3} for the RB5 solution sample which has been decomposed by 90%); x is the length along the direction of the diffusion (estimate 1×10^{-7} m).

Residence time distribution (RTD) for the measuring apparatus is shown in Figure 3.6 for the flow at 5 ml/min and in Figure 3.7 for the flow at 10 ml/min. The average residence time is 1.16 min for the 5 ml/min flow and 0.64 min for the 10 ml/min flow. Reynolds numbers of the 5 ml/min flow and 10ml/min flow are 10.82 and 21.64, which indicates that the flows at 5 ml/min and 10 ml/min in the glass tube reactor are laminar flow.

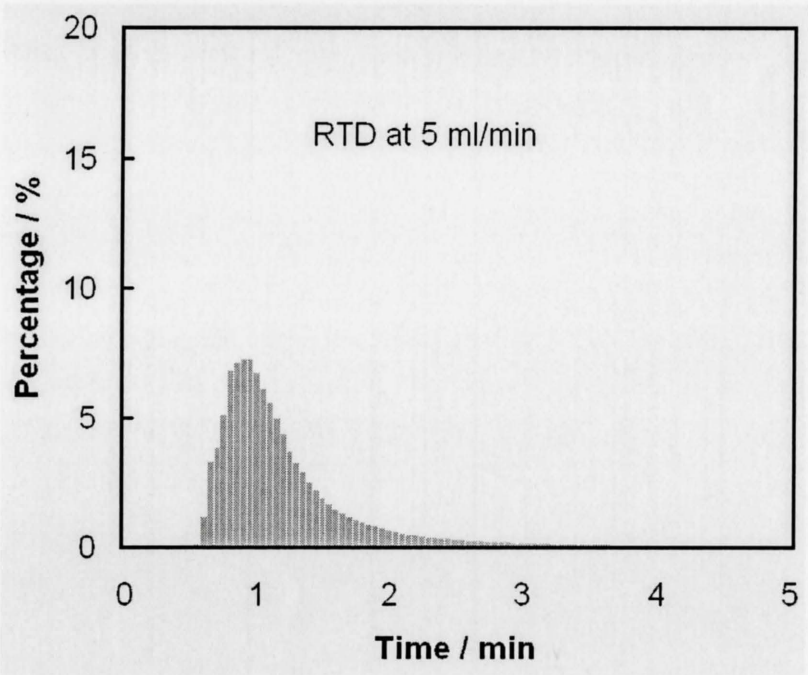

Figure 3.6 RTD of the decomposition measuring apparatus, flow rate=5 ml/min

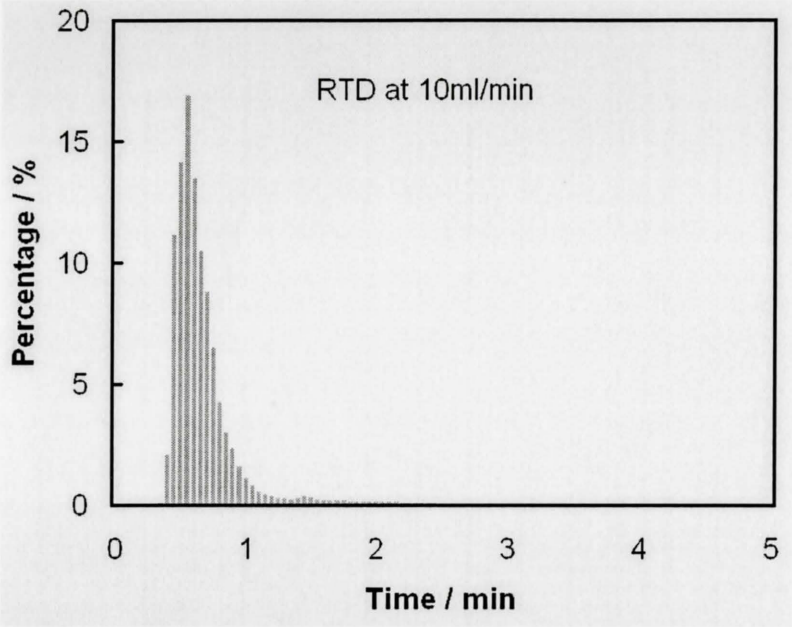

Figure 3.7 RTD of the decomposition measuring apparatus, flow rate=10 ml/min

3.1.2.2 Adsorption of RB5 at TiO_2 coated paper

The influence of the pH of RB5 solution was studied since the surface charge of TiO_2 coated paper varies significantly at different pH. Figure 3.8 shows the adsorption of RB5 molecules at the TiO_2 surface. The adsorption increased when pH decreased. The adsorption of RB5 at blank filter paper was also measured and no adsorption was obtained in the experiments.

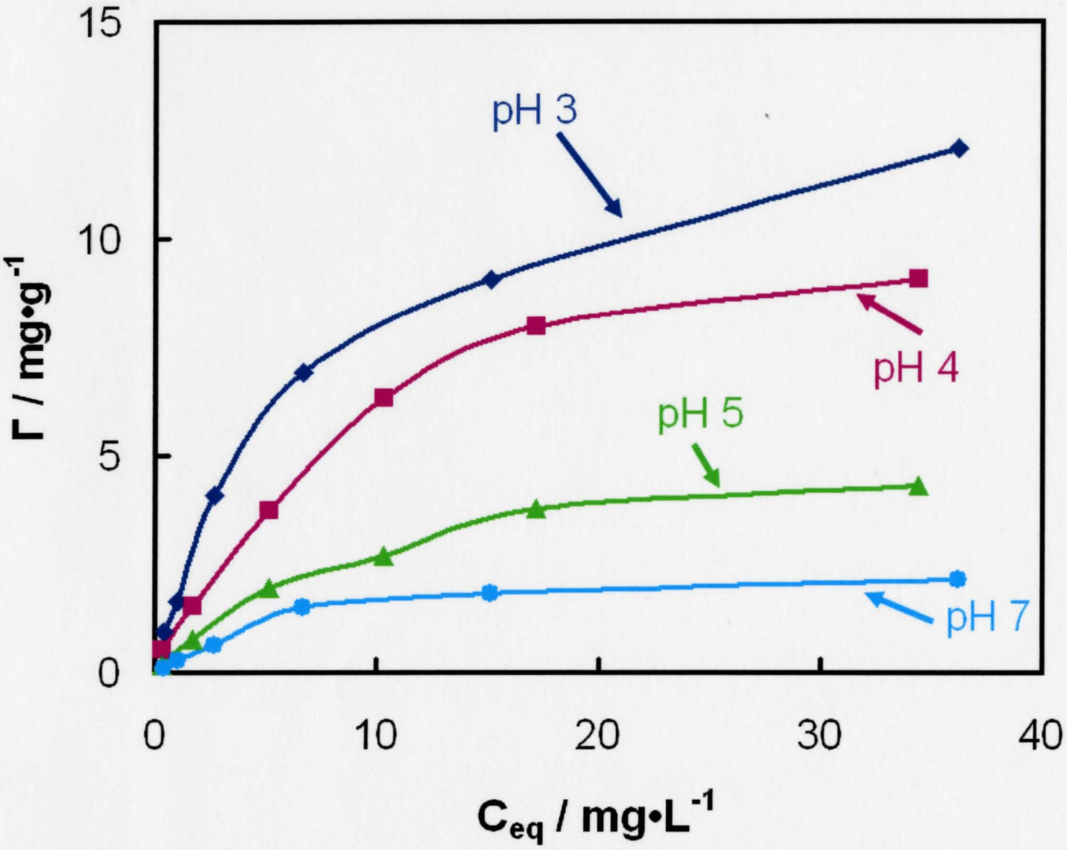

Figure 3.8 Adsorption of RB5 molecules on the TiO_2 surface at four different pH.

Figure 3.9 shows that the effect of ionic strength is dependent on pH. When the pH of RB5 solution was 3, which indicates TiO_2 surface is positive, the adsorption of 1 M NaCl sample dropped by over 85% compared with the no salt sample. But at pH7, the presence of electrolytes had little influence on the adsorption.

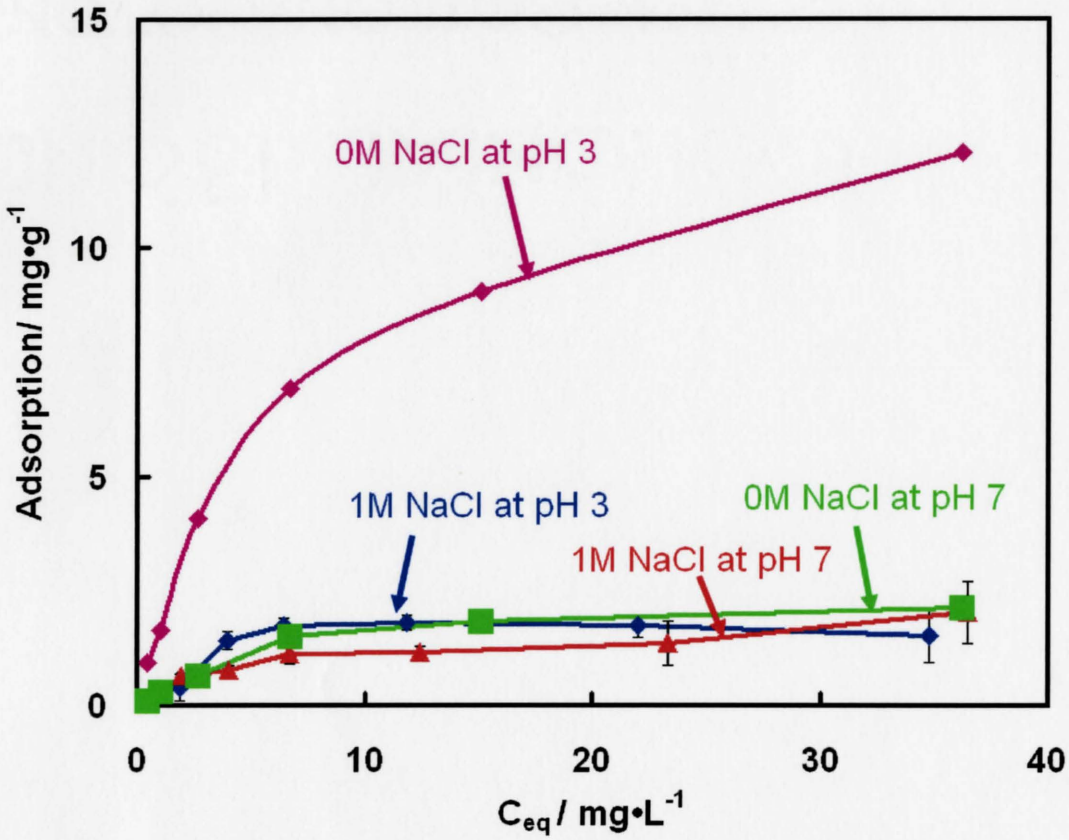

Figure 3.9 ***Adsorption of RB5 molecules on the TiO_2 surface at different ionic strength.***

The electrophoretic mobility values of TiO_2 at three different conditions were measured (shown in Figure 3.10). When RB5 molecules were adsorbed onto the surface of the TiO_2 particle, the surface charge of TiO_2 became negative. After the TiO_2 particles had been irradiated for 6 hours, the RB5 molecules that were adsorbed on the TiO_2 surface were decomposed and the surface charge of TiO_2 became positive again. That means the ability of adsorbing RB5 molecules would be recovered for TiO_2 after the adsorbed RB5 molecules were decomposed.

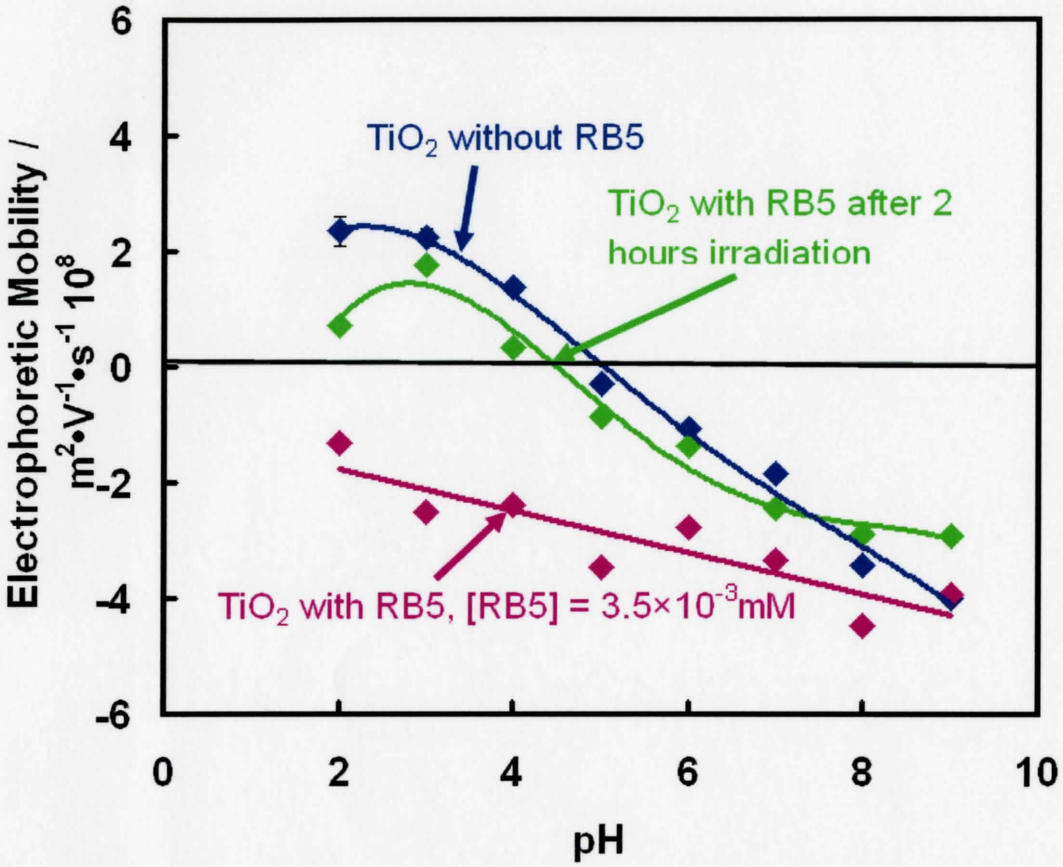

Figure 3.10 Electrophoretic mobility of TiO_2 particles at three different conditions. ($[NaCl]=5\times10^{-3}M$)

3.2 Factors in the decomposition of RB5 solution

The effect of the dye decomposition by TiO_2 depends on two aspects: (1) the concentration of the hydroxyl free radicals and (2) the concentration of dye near the TiO_2 surface. In the following content of Chapter 3.2, the effects of pH, ionic strength, UV intensity, temperature and flow rate will be shown.

3.2.1 Effect of pH

The influence of the pH of the RB5 solution was studied. Figure 3.11 shows the RB5 decomposition at four different pH values. The decomposition rate of RB5 in the strong acidic solution is significantly higher than that in the weak acidic or neutral solution.

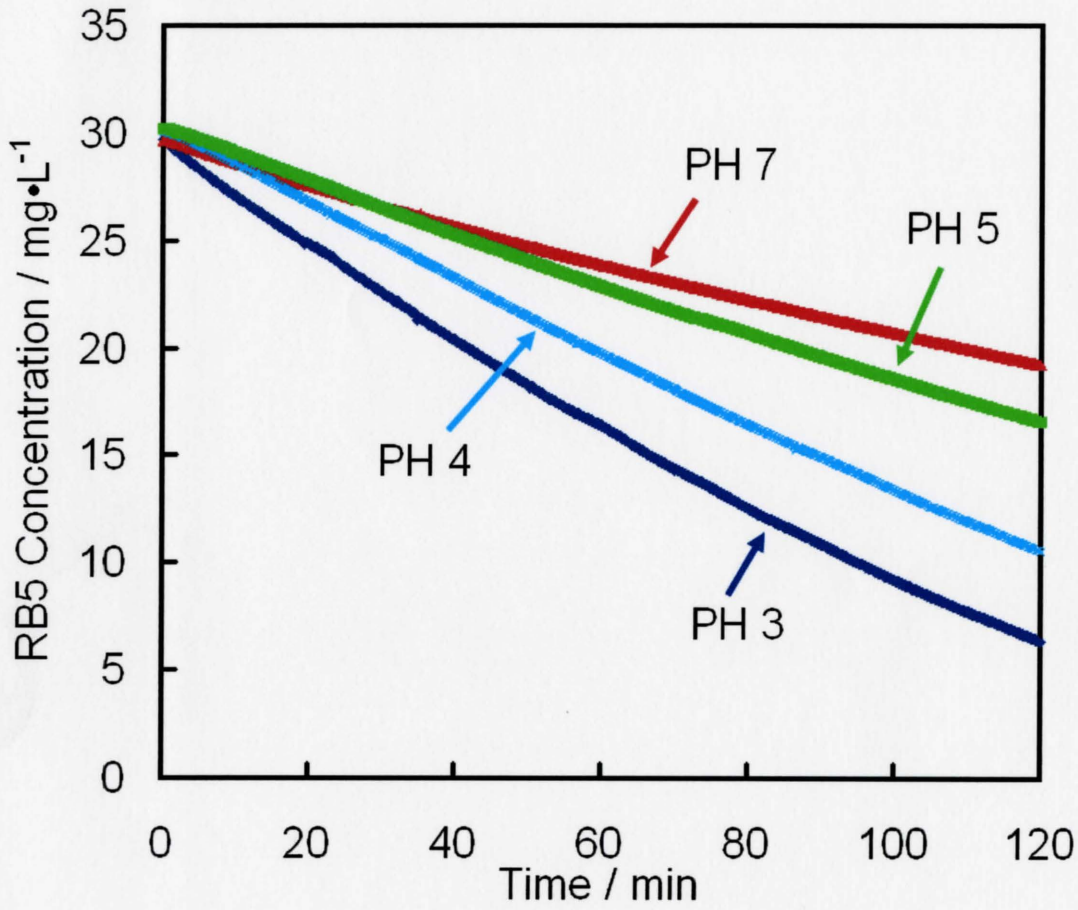

Figure 3.11 Decomposition of RB5 solution at different pH (TOP10, UV intensity 1.02mW/cm^2, [NaCl]=0M, flow rate 5ml/min, room temperature)

3.2.2 Effect of Ionic strength

The influence of the ionic strength was measured at five different NaCl concentrations. Figure 3.12 shows the decomposition of the RB5 solution at different ionic strength levels. The decomposition rate decreased significantly with the presence of the electrolytes.

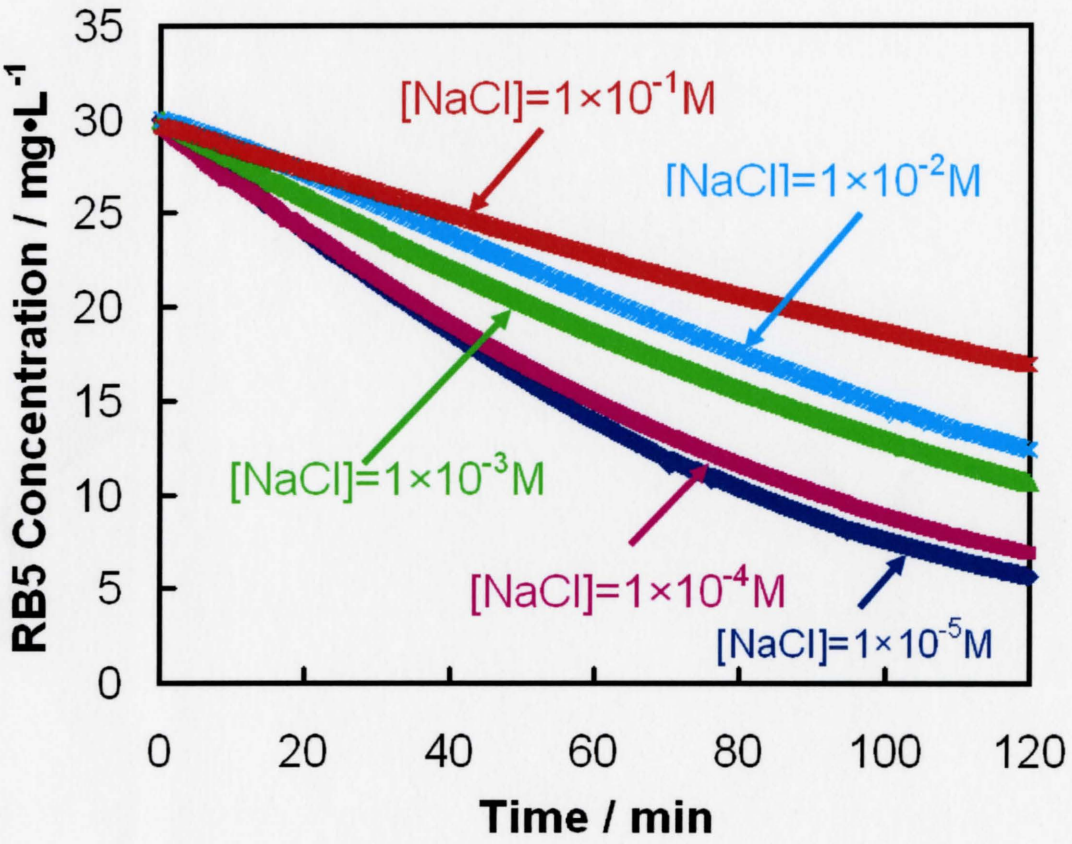

Figure 3.12 Decomposition of RB5 solution at different ion strength. (TOP10, UV intensity 1.02mW/cm^2, pH3, flow rate 5ml/min, room temperature)

3.2.3 Effect of UV intensity

The influence of the UV intensity was studied at four different UV intensities. Figure 3.13 shows the decomposition of RB5 solution with UV irradiation of different intensities. The decomposition rate is proportional to UV intensity.

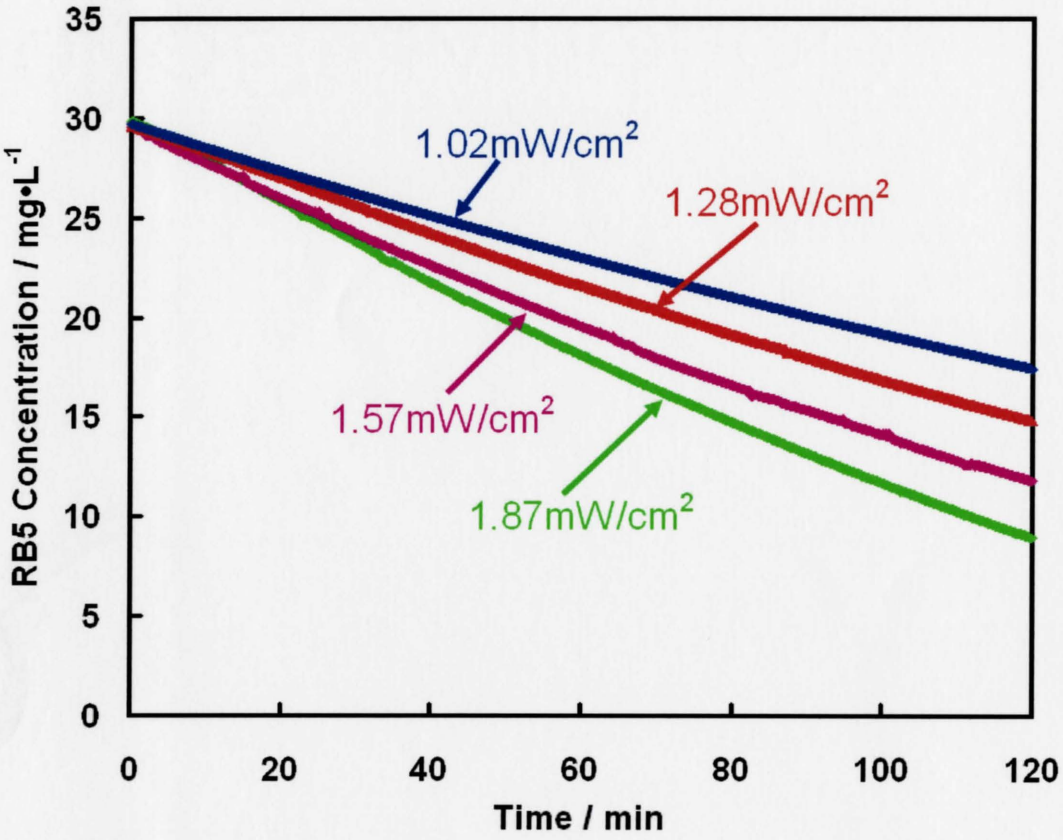

Figure 3.13 Decomposition of RB5 solution at different UV intensities / mW·cm^{-2}. (TOP10, pH7, flow rate 5ml/min, room temperature)

3.2.4 Effect of Temperature

The influence of temperature was measured at five temperatures each pH. Figure 3.14 and Figure 3.15 shows the temperature can affect the decomposition rate both at pH 3 and pH 7. When temperature increased, the decomposition rate increased at both pH 3 and pH 7.

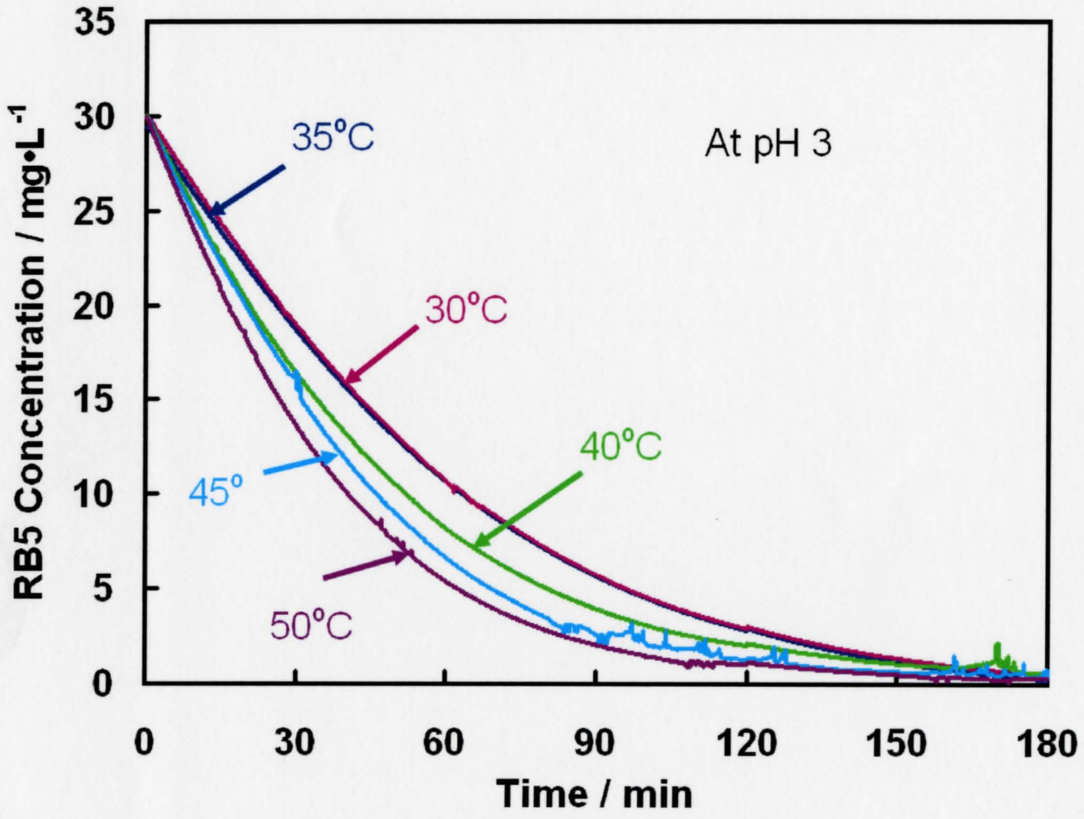

Figure 3.14 Decomposition of RB5 solution at different temperatures. (TOP10, UV intensity 1.86mW/cm^2, pH3, flow rate 5ml/min)

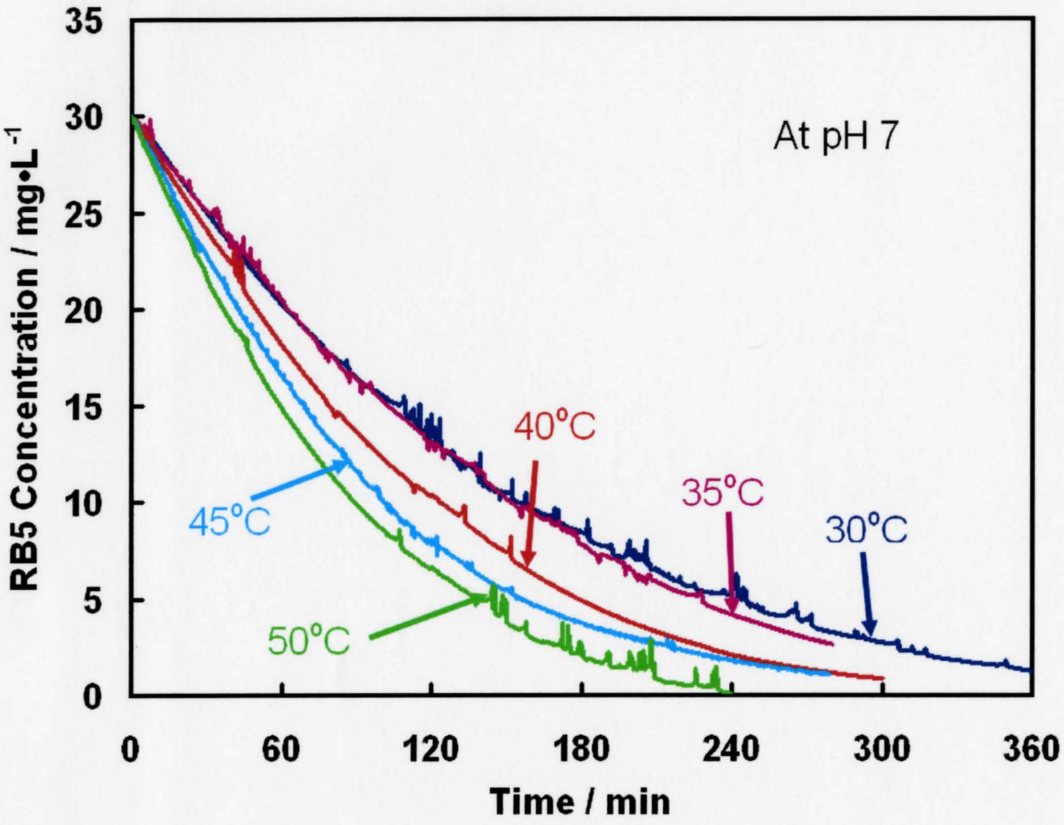

Figure 3.15 Decomposition of RB5 solution at different temperatures. (TOP10, UV intensity 1.86mW/cm^2, pH7, flow rate 5ml/min)

3.2.5 Effect of Flow rate and TiO_2 amount on the paper

The effect of solution flow rate was measured at two different flow rates. Figure 3.16 shows the concentration changes of the RB5 solution at two different flow rates. The flow rate had little influence on the RB5 decomposition rate.

The influence of the TiO_2 amount on the paper was also studied. No significant difference was found by using different TiO_2 coated paper samples (TOP5, TOP10 and TOP20).

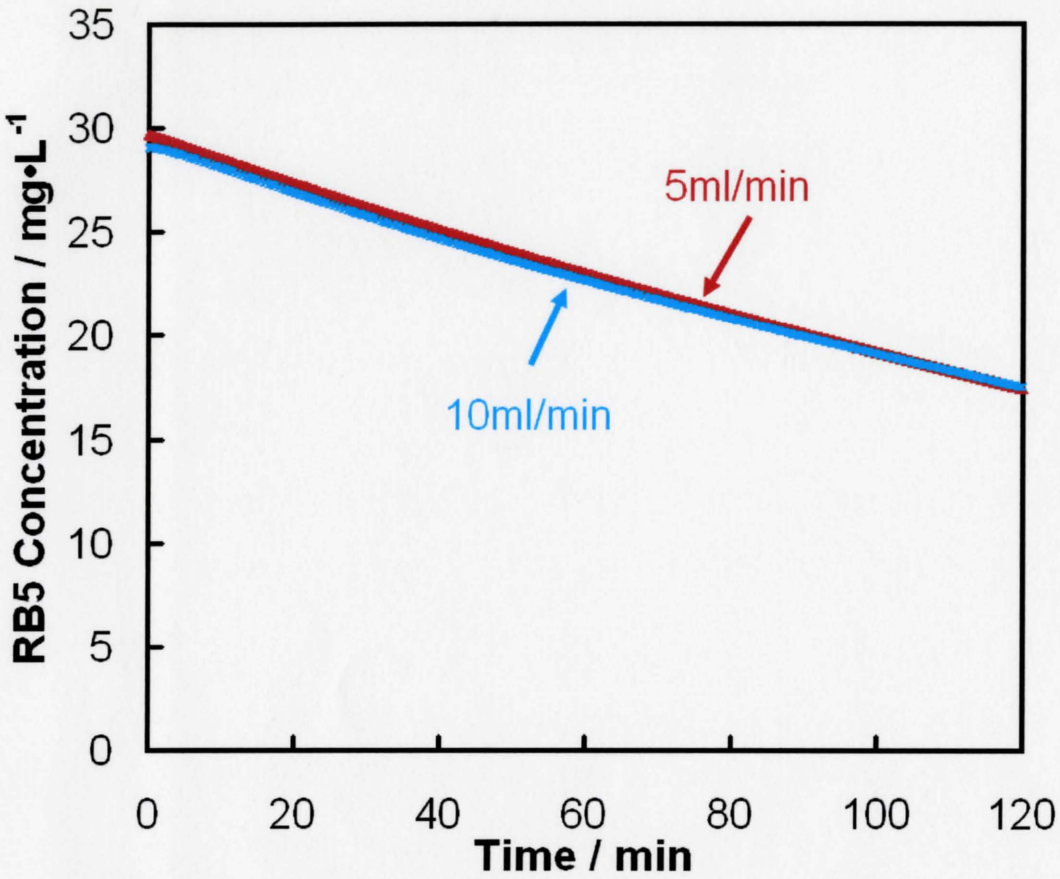

Figure 3.16 Decomposition of RB5 solution at two different flowing rate. (TOP10, UV intensity 1.02mW/cm^2, pH7, flow rate 5ml/min)

3.3 The presence of the intermediate products

3.3.1 The introduction of the intermediate products

Intermediate products were obtained when the concentration of NaCl was over 1M in the RB5 solution. Figure 3.18 shows the absorbance spectra of the RB5 solution (0M NaCl), which was irradiated under UV light for different times. The decomposition of the RB5 solution can be monitored at three typical peaks of 313nm, 391nm and 597nm.

In this experiment, no new distinctive peaks appeared and the spectrum of the RB5 solution irradiated overnight indicated that the RB5 molecules had been oxidized into simple molecules such as CO_2 and H_2O. The same experiment was done by using the RB5 solution with 1M NaCl. The spectra (Figure 3.19) show the three typical peaks of the RB5 solution decrease after different time irradiations whereas three new distinctive peaks at 278 nm, 359 nm and 521 nm appeared. That indicates the RB5 molecules were not decomposed completely but into some intermediate products during the process of the photocatalytic decomposition. The intermediate products were not decomposed even after being irradiated under UV light for 24 hours. Figure 3.17 shows the pictures of RB5, intermediate products and final products solutions.

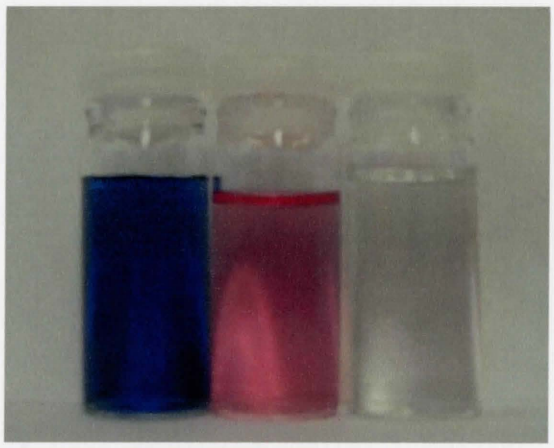

Figure 3.17 The picture of the RB5 (left), intermediate products (middle) and final products solutions (right).

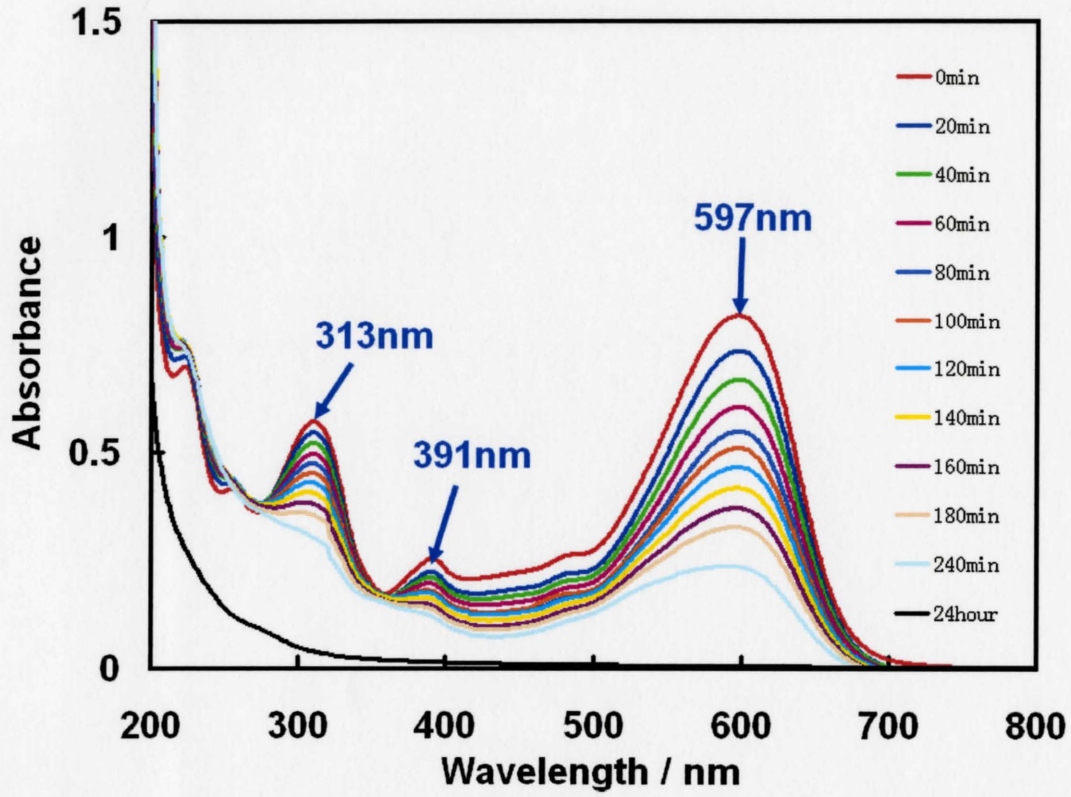

Figure 3.18 ***UV-visible spectra of the RB5 solutions irradiated under UV light for 0 min, 20 min, 40 min, 60 min, 80 min, 100 min, 120 min, 140 min, 160 min, 180 min, 240 min and 24 hour. ([NaCl]=0M, TOP10, UV intensity 1.02mW/cm^2, pH7, flow rate 5ml/min)***

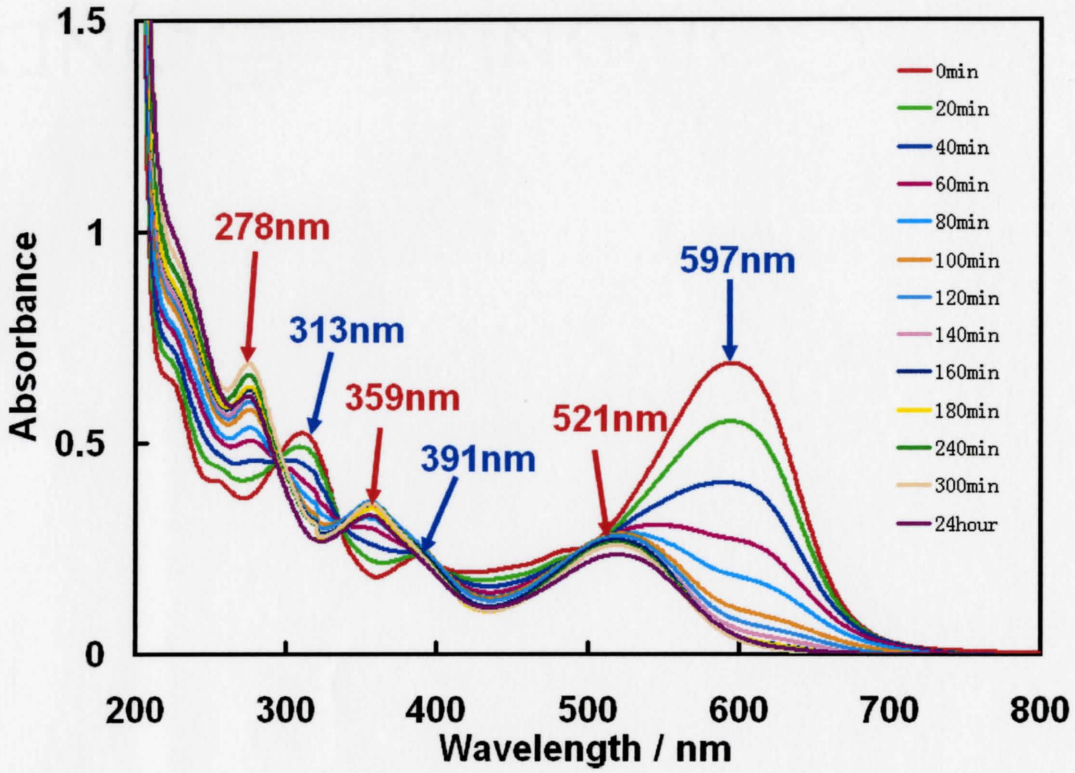

Figure 3.19 ***UV-visible spectra of the RB5 solutions irradiated under UV light for 0 min, 20 min, 40 min, 60 min, 80 min, 100 min, 120 min, 140 min, 160 min, 180 min, 240 min, 300 min and 24 hour. ([NaCl]=1M, TOP10, UV intensity 1.02mW/cm^2, pH7, flow rate 5ml/min)***

3.3.2 The adsorption of intermediate products at TiO_2 surface

The adsorption of intermediate products onto TiO_2 was measured at pH 3 and pH 7 since the adsorption is so important for the decomposition. No salt samples, 0.1M NaCl samples and 1M NaCl samples were prepared at the two pH levels. The adsorption values (Figure 3.20) changes very little when the concentration of NaCl was less than 0.1M even

though the pH had been changed. But the adsorption dropped to near 0 when the concentration of NaCl reached 1M.

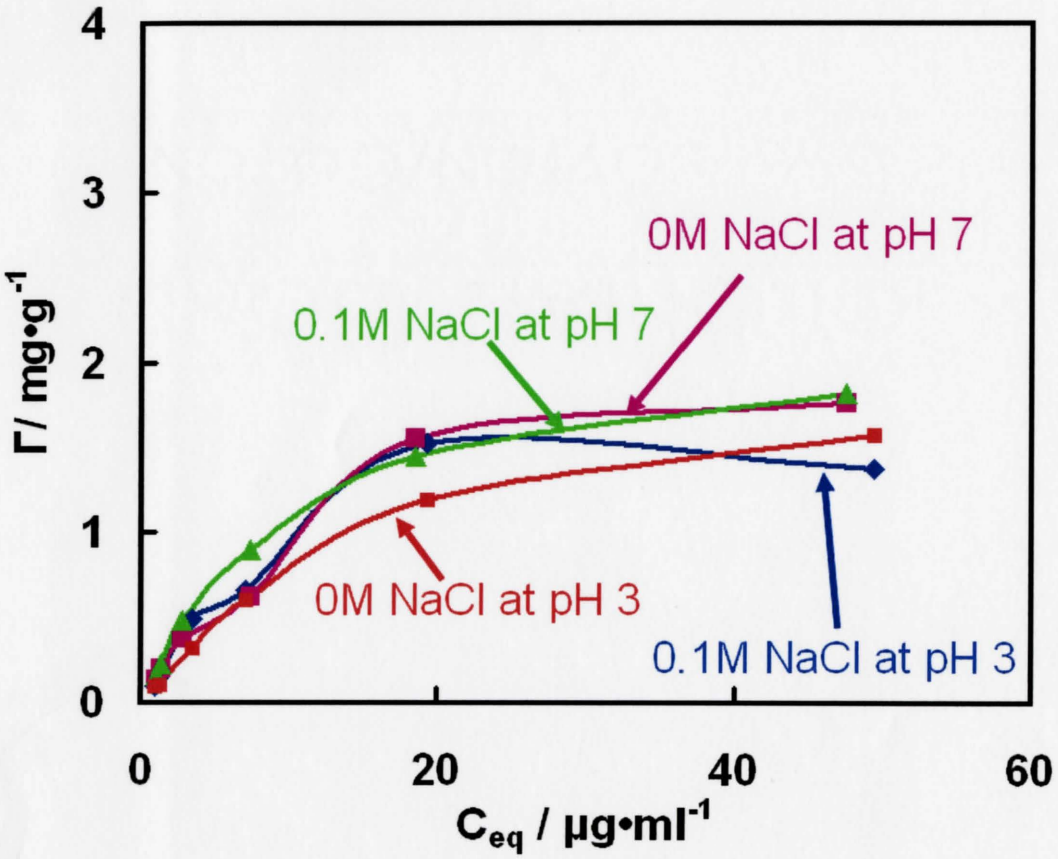

Figure 3.20 Adsorption of the intermediate products on the TiO_2 particles.

3.3.3 The decomposition of intermediate products

The decomposition of intermediate products was measured under four conditions (Figure 3.21). It is interesting that the decomposition rate increased when the

concentration of NaCl was increased from 0 to 0.1M whereas pH had little influence on the decomposition rate.

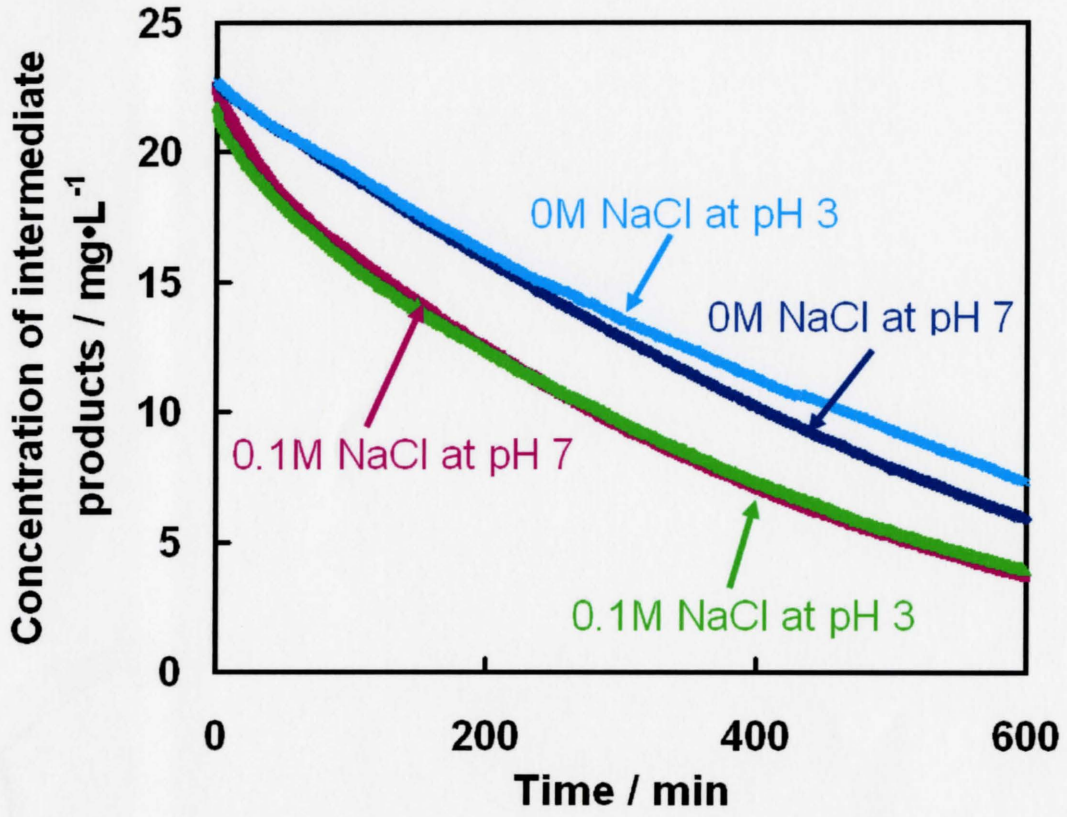

Figure 3.21 ***Decomposition of intermediate products solution on four conditions. (TOP10, UV intensity 1.02mW/cm^2, flow rate 5ml/min, room temperature)***

4 Discussion

4.1 The stability of TiO_2 at paper surface

In our experimental results, TiO_2 particles adhered to the surface of the filter paper when pH was below 7. But when the pH was above 8, TiO_2 desorbed from the paper surface. The pH-controllable behavior may caused by two reasons. The first is that the interaction between paper fibers and TiO_2 particles are changed by altering pH. The second is that the polymeric retention aids are invalidated, such as swelled, at high pH.

Usually, the porosity and hydrophobicity of the paper samples is considered very important in controlling the particle dispersion on the paper surface [3, 15].The filter paper (Type 4, Whatman®) used in the experiments has a high particle retention (22-25 μm). The strong deposition of colloid particles cannot occur at the paper surface without polymeric retention aids[70]. If the first reason is right, the retention aids and other additives should modify the negatively charged pulp fibers. In DLVO theory, the deposition occurs if the colloid particles are oppositely charged. The surface charge of TiO_2 changed as pH was changed. When pH $\leq$ 5, the surface of TiO_2 is positively charged or contains no charges. On this condition, TiO_2 particles can adhere to the fiber surface. When pH is above 5, the electrostatic interaction becomes negative and the adsorption of TiO_2 at the paper surface is weakened. TiO_2 should be desorbed from the paper surface. But in our experiments, no desorption of TiO_2 was detected at pH 7. Furthermore, electrolyte can also affect the electrostatic interaction in DLVO theory. But no TiO_2 was detected at a NaCl concentration of 1M at pH 7 and at pH 3. So the influence of pH is not caused by the electrostatic interaction.

From the foregoing discussions, the invalidation of polymeric retention aids should be the reason why TiO_2 is desorbed at high pH. However, the specific reason cannot be studied by now due to the lack of information.

4.2 Factors influencing the TiO_2 photocatalytic decomposition rate

Four factors (pH, ionic strength, UV intensity and temperature) could affect the TiO_2 photocatalytic decomposition rate in our experiments.

The effect of pH and ionic strength can be explained by DLVO theory (Figure 4.1). RB5 molecules are negative when pH is below 7. In strong acidic solution, TiO_2 layer turns positive and the electrostatic attraction made more RB5 molecules attached on the surface of TiO_2 layer than in other situations. RB5 molecules were concentrated at the TiO_2 surface and thus were easily attacked by the free radicals present nearby. In weak acidic or neutral solution, the TiO_2 layer turns negatively charged and no electrostatic attraction exits. In this situation, only a little part of RB5 molecules is attached on the TiO_2 layer and the decomposition becomes difficult. The addition of electrolyte should weaken the electrostatic interaction between RB5 molecules and TiO_2 layer. Therefore the adsorption is weakened and the decomposition rate is decreased. The effect of pH and ionic strength could be concluded as affecting the electrostatic interaction and adsorption between the RB5 molecules and the TiO_2 layer.

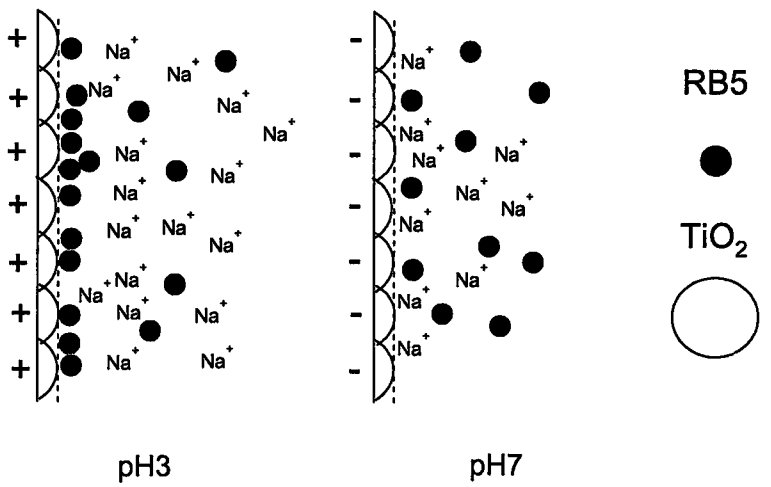

Figure 4.1 Adsorption of Rb5 at two different pH following DLVO theory.

Increasing UV intensity can increase the decomposition rate. With high UV intensity, the number of free radicals and active holes becomes high at the surface of TiO_2 and the organic dyes can be oxidized more effectively. It has reported that the decomposition rate is proportional to the UV intensity below 20 mW/cm^2 and is proportional to the square root of the UV intensity above 20 mW/cm^2 [71]. Our experimental data repeated their data.

The decomposition rate is temperature sensitive in our experiments. It has reported that TiO_2 photocatalytic rate is weakly temperature-sensitive[72]. The dependence is from the activation energy. The values of activation energies are 5-20 kJ/mol depending on the type of organic compounds[73]. This is close to the activation energy of hydroxyl free radicals reactions. That also indicates that the oxidation is mainly governed by the hydroxyl free radicals reactions[74].

4.3 Intermediate products

Intermediate products were found in the experiments of TiO_2 photocatalytic decomposition of RB5 solution, although it has been predicted before[63]. The big change in adsorption is believed to be the reason why intermediate products are obtained in the decomposition of the RB5 solutions. When a large amount of electrolyte is added into the solution, the adsorption of intermediate products becomes quite low and the desorption rate of intermediate products becomes quite high. The intermediate-product molecules are desorbed from the TiO_2 surface before they are decomposed further.

Unfortunately, the structure of intermediate products has been obtained. But the adsorption at TiO_2 surface and the decomposition by TiO_2 photocatalysis was studied. Usually, pH and ionic strength have little influence on the adsorption of intermediate products. But when the concentration of NaCl reached 1M, the adsorption dropped to around zero. The effect of electrolyte cannot be explained by any theories. The reason why adding NaCl can increase the decomposition rate can't be obtained either.

5 A kinetic model for the photocatalytic decomposition of RB5 solutions

The effect of the RB5 adsorption was studied by altering pH and ionic strength. The decomposition rate always increases with the RB5 adsorption increases. To simplify the model, it is assumed that only the RB5 molecules adsorbed on the TiO_2 surface can be decomposed. Free radicals cannot move too far away from TiO_2 surface due to its short lifetime. Also, the active holes (h^+) at TiO_2 surface can decompose RB5 molecules. Therefore, RB5 molecules are decomposed mainly at the TiO_2 surface rather than in the bulk. The decomposition rate is dependent on the adsorption of RB5 molecules at the TiO_2 surface. Figure 5.1 shows the decomposition of the RB5 solution on the surface of TiO_2 coated paper at two different pH.

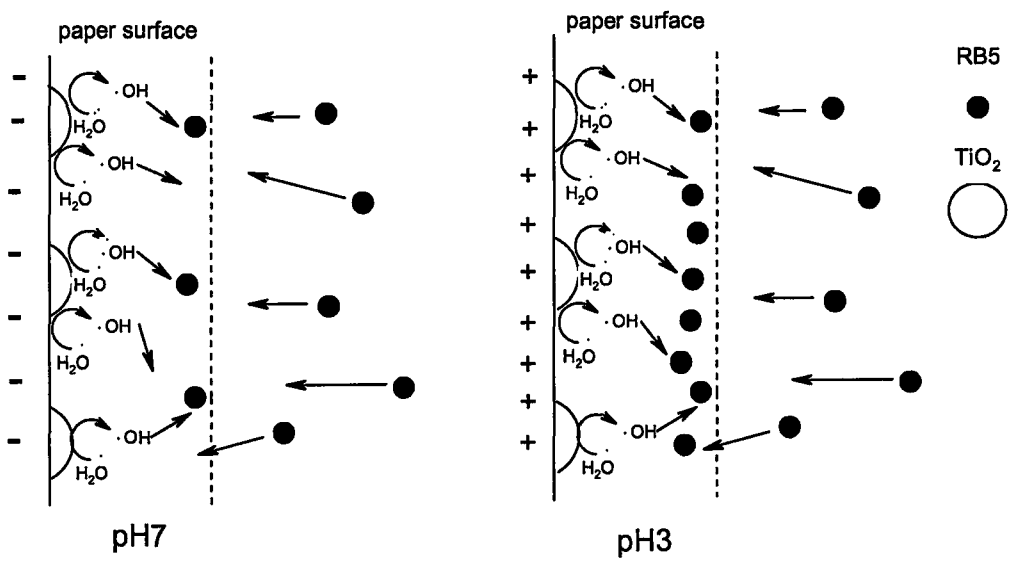

Figure 5.1 The reactions at the surface of the TiO_2 coated paper.

From Figure 5.1, the decomposition rate should be controlled by either diffusion rate or the reaction rate. For the 1×3 cm TiO_2 coated paper sample, the diffusion rate from the solution to the TiO_2 surface can reach 2.67×10^{-9} kg/s when the concentration of RB5 solution is 3 mg/L (Chapter 3.1.2.1). The true diffusion rate is larger than 2.67×10^{-9} kg/s because the flow can also increase the diffusion rate. The decomposition rate is around 5×10^{-11} kg/s at the optimum conditions by now. The diffusion rate is much larger than the decomposition rate. Therefore, the adsorption is at equilibrium state in the decomposition process.

From the foregoing discussion, two critical aspects could be identified in the case of the photocatalytic decomposition of RB5: (1) the adsorption is at equilibrium state and has strong influence in the decomposition rate (2) intermediate state exits and intermediate products can be obtained at some conditions (Chapter 3.3). Therefore, the decomposition model should follow the Langmuir adsorption and have a two-step reaction. Figure 5.2 shows RB5 molecule decomposition model.

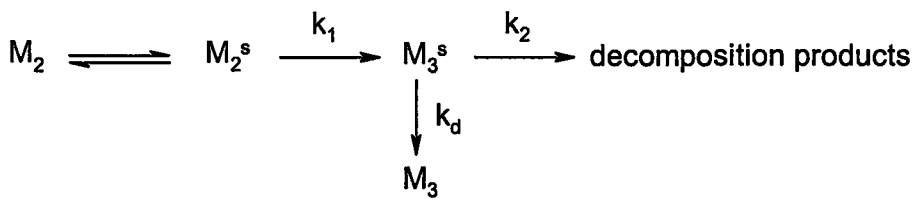

Figure 5.2 ***The model of RB5 decomposition. (M_2: RB5 molecule in the bulk, M_2^s: the RB5 molecule at the TiO_2 surface, M_3: intermediate products molecule desorbed from the TiO_2 surface, M_3^s: intermediate products***

molecule at the TiO_2 surface, k_1 , k_2 : the reaction constant, k_d: the desorption constant.)

To solve this model, Langmuir model (Equation 5.1) is used to describe the adsorption of RB5 and the adsorption of intermediate products. All the decomposition experiments did not start until the coated was stable and the adsorption of RB5 is quite strong. So it is reasonable to set the adsorption at the equilibrium state.

$$\frac{1}{n_2^s} = \frac{1}{n^s \bullet b \bullet C_{eq}} + \frac{1}{n^s} \tag{5.1}$$

The reactions of decomposing the RB5 molecules and the intermediate products are both first-order[63]. The expression for the first step of the reaction can be written as Equation 5.2.

$$\frac{dC_2}{dt} = -k_1 n_2^s \tag{5.2}$$

Using Equation 3.9, the expression can be written as Equation 5.3.

$$\frac{C_2 - C_2(0)}{n^s} + \frac{1}{n^s b} \ln \frac{C_2}{C_2(0)} = -k_1 t \tag{5.3}$$

Where $C_2(0)$ is the bulk concentration of RB5 at the starting point. For the intermediate products, the expression can be written as Equation 5.4.

$$\frac{dn_3^s}{dt} = k_1 n_2^s - k_2 n_3^s - k_d n_3^s \tag{5.4}$$

The similar decomposition experiments were started from intermediate products and the reaction scheme is shown in Figure 5.3. k_2 can be calculated from the decomposition of the intermediate products and the adsorption of the intermediate products (Equation 5.5 or Equation 5.6). Table 5.1 shows the parameters b, n^s and k_2.

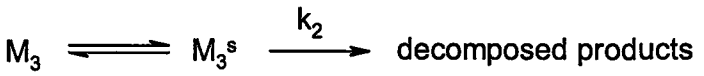

Figure 5.3 The model of the intermediate products decomposition.

Table 5.1 Parameters for the intermediate products decompositions. (The molecular weight is assumed as 500 Daltons)

	b /g·mol^{-1}	$n^s/\times10^3$ mol·g^{-1}	$k_2/\times10^{-5}$ min^{-1}	R^2 for the adsorption	R^2 for the decomposition
pH 3, 0M NaCl	0.0234	3.82	5.6	0.988	0.998
pH 3, 0.1M NaCl	0.0189	6.33	4.8	0.981	0.994
pH 7, 0M NaCl	0.0241	5.07	5.8	0.964	0.997
pH 7, 0.1M NaCl	0.0294	5.44	5.0	0.985	0.993
Average	-	5.17	5.3	-	-
SD	-	1.05	0.476	-	-

$$\frac{dC_3}{dt} = -k_1 n_3^s \tag{5.5}$$

$$\frac{C_3 - C_3(0)}{n^s} + \frac{1}{n^s b} \ln \frac{C_3}{C_3(0)} = -k_2 t \tag{5.6}$$

For the RB5 decomposition, the adsorption of intermediate products is as strong as RB5, when the concentration of NaCl $\leq$0.1M. So the desorption rate is much lower than the reaction rate and the expression can be written as Equation 5.7.

$$\frac{dn_3^s}{dt} = k_1 n_2^s - k_2 n_3^s \tag{5.7}$$

For the intermediate products, the accumulation is very fast at first, but the equilibrium for the accumulation-reaction should be reached after a short time. The equilibrium for the RB5 adsorption has been demonstrated above and the steady state can be considered for the adsorption of intermediate products. So Equation 5.7 can be rewritten as Equation 5.8.

$$\frac{dn_3^s}{dt} = k_1 n_2^s - k_2 n_3^s = 0 \tag{5.8}$$

In this situation, the decomposition rate can be written as Equation 5.9. All the parameters are shown in Table 5.2.

$$r = k_2 n_3^s = k_1 n_2^s = \frac{dC_2}{dt} \tag{5.9}$$

When the concentration of NaCl ≥1M, the desorption of intermediate products became quite high and could not be ignored. The expression of the decomposition rate r and the desorption rate r_d can be written as Equation 5.10 and 5.11.

Table 5.2 Parameters for the RB5 decompositions.

	b / $g \cdot mol^{-1}$	$n^s / \times 10^3$ $mol \cdot g^{-1}$	$k_1 / \times 10^{-5}$ min^{-1}	R^2 for the adsorption	R^2 for the decomposition
pH 3	0.200	11.16	2.4	0.988	0.998
pH 4	0.220	7.32	2.7	0.989	0.999
pH 5	0.0719	6.78	2.7	0.999	0.999
pH 7	0.0223	10.91	2.4	0.992	0.998
Average	-	9.04	2.55	-	-
SD	-	2.31	0.173	-	-

$$r = k_2 n_3^s = k_2 \frac{k_1}{k_2 + k_d} n_2^s = \frac{k_2}{k_2 + k_d} \frac{dC_2}{dt} \qquad (5.10)$$

$$r_d = k_d n_3^s = k_d \frac{k_1}{k_2 + k_d} n_2^s = \frac{k_d}{k_2 + k_d} \frac{dC_2}{dt} \qquad (5.11)$$

6 Conclusions

TiO_2 photochemistry has been investigated for around 35 years. The photocatalytic decomposition and photocatalytic disinfection have been studied by a large number of research groups. However the specific mechanism of the photocatalytic decomposition is not clear. Our work demonstrates the effects of pH, ionic strength, UV intensities, temperature and flow rates on the decomposition rate. A kinetic model of the photocatalytic decomposition was also developed.

The major contributions of this works are:

1. Intermediate products were detected in the process of TiO_2 photocatalytic decomposition of RB5 solution. This discovery proved the prediction of intermediate products[63] and proved the suitability of two-step first-order model.
2. A new kinetic model was built. This model followed the principles of LH model and two-step first-order model. The desorption of intermediate products was also added into the model.
3. pH, ionic strength, UV intensity and temperature have influences on TiO_2 photocatalytic decomposition rate. The decomposition rate is high at low pH and low ionic strength. Increasing either UV intensity or temperature can increase the decomposition rate.
4. Adsorption properties of TiO_2 coated paper are dependent on the surface charge of TiO_2 particles. The stability of TiO_2 coated paper is determined by the properties of retention aids.

5. A continuously measuring apparatus was built to detect the real-time changes of TiO_2 photocatalytic decomposition.

For further work, the isolation of intermediate components is needed. The structural information for each component of the intermediate products is also needed to develop the mechanism of TiO_2 photocatalytic decomposition. TiO_2 coated paper is an attractive product as it can be recycled in the application and needs no more energy except that from the sunlight. Clear photocatalytic decomposition will make it more effective in the future application.

7 Appendix

All following calculation was performed by excel (Microsoft).

7.1 Decomposition of intermediate products

Objective: demonstrate the equations which predict TiO_2 photocatalytic decomposition for intermediate products and the calculation of the reaction rate k_2.

From Langmuir model

$$\frac{1}{n_3^s} = \frac{1}{n^s \bullet b \bullet C_{eq}} + \frac{1}{n^s}$$

n^s and b can be calculated from the slope $1/ n^s b$ and the y intercept $1/n^s$ of the linear trendline . Testing Langmuir model for the adsorption of intermediate products

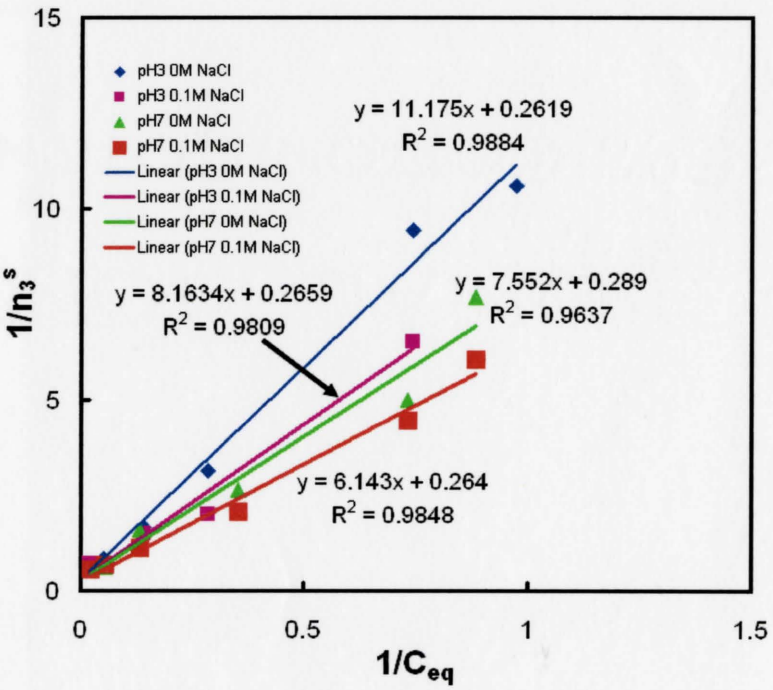

The adsorption data fit Langmuir model well. The results of b and n^s of the calculation are shown in Table 5.1.

From decomposition model

$$\frac{C_3 - C_3(0)}{n^s} + \frac{1}{n^s b} \ln \frac{C_3}{C_3(0)} = -k_2 t$$

k_2 is calculated as the average of the k_2 of each data point. Testing the decomposition model for intermediate products

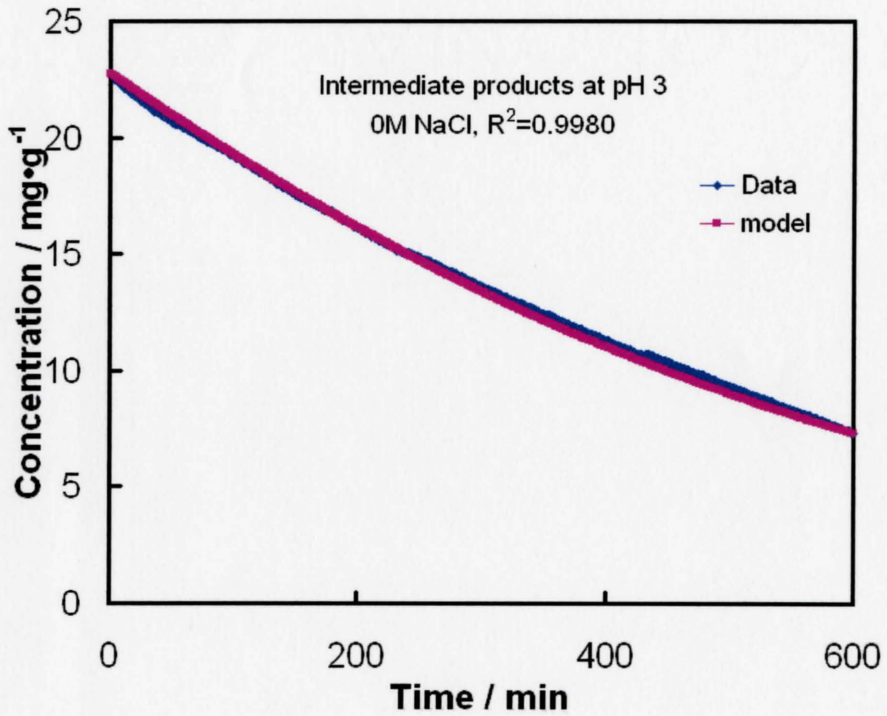

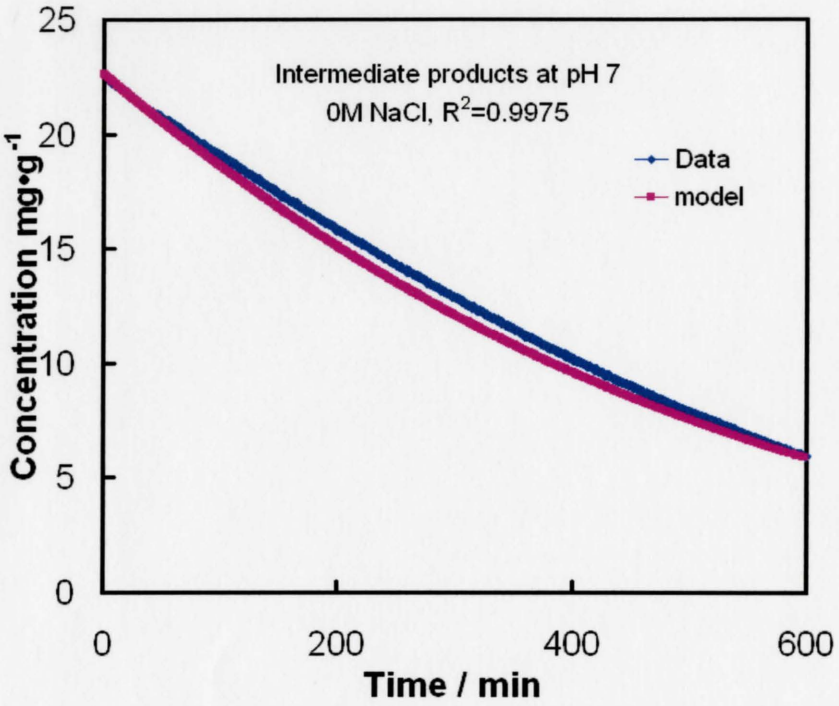
Intermediate products at pH 7
0M NaCl, R^2=0.9975
Data
model
Concentration mg•g-1
Time / min
0
5
10
15
20
25
0
200
400
600

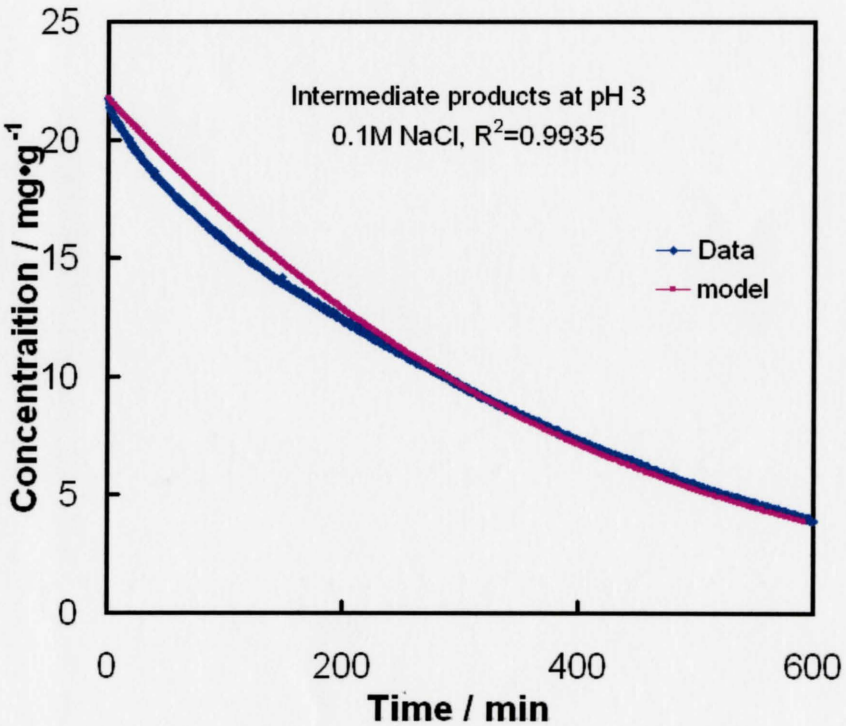
Intermediate products at pH 3
0.1M NaCl, R^2=0.9935
Data
model
Concentraition / mg•g-1
Time / min
0
5
10
15
20
25
0
200
400
600

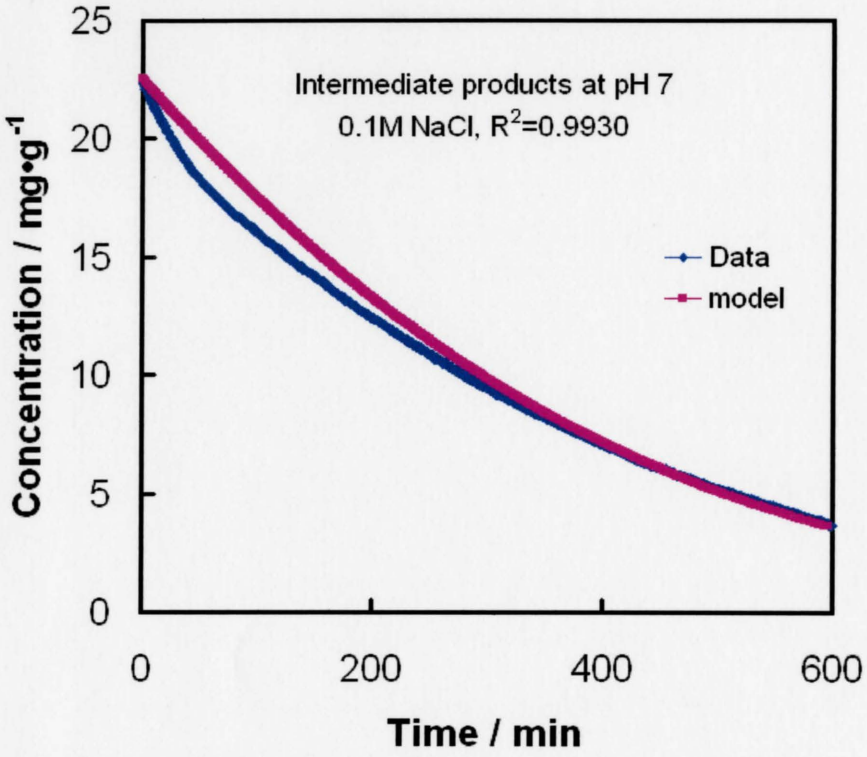

The fit is very good. And the results of k_2 are shown in Table 5.1.

7.2 Decomposition of RB5

Objective: demonstrate the equations which predict TiO_2 photocatalytic decomposition for RB5 and the calculation of the reaction rate k_1.

From Langmuir model

$$\frac{1}{n_2^s} = \frac{1}{n^s \bullet b \bullet C_{eq}} + \frac{1}{n^s}$$

n^s and b can be calculated from the slope $1/ n^s b$ and the y intercept $1/n^s$ of the linear trendline. Testing Langmuir model for the adsorption of RB5

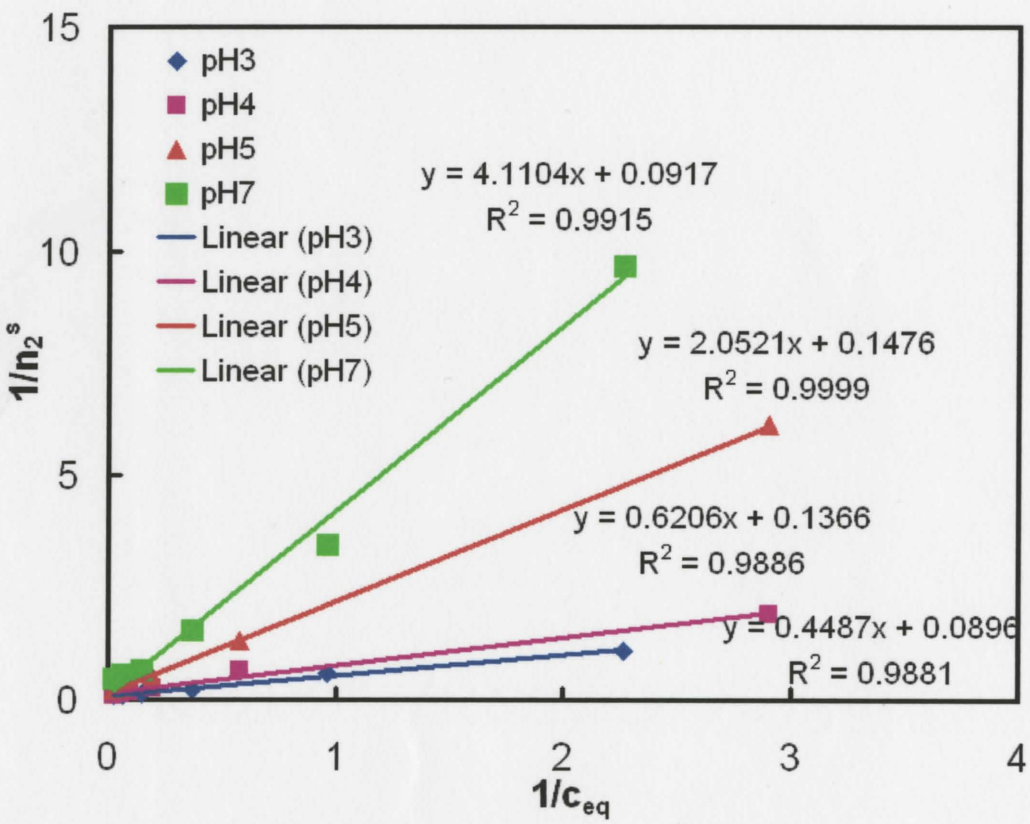

The adsorption data fit Langmuir model well. The results of the calculation are shown in Table 5.2.

From decomposition model

$$\frac{C_2 - C_2(0)}{n^s} + \frac{1}{n^s b} \ln \frac{C_2}{C_2(0)} = -k_1 t$$

k_1 is calculated as the average of the k_1 of each data point. Testing the decomposition model for RB5

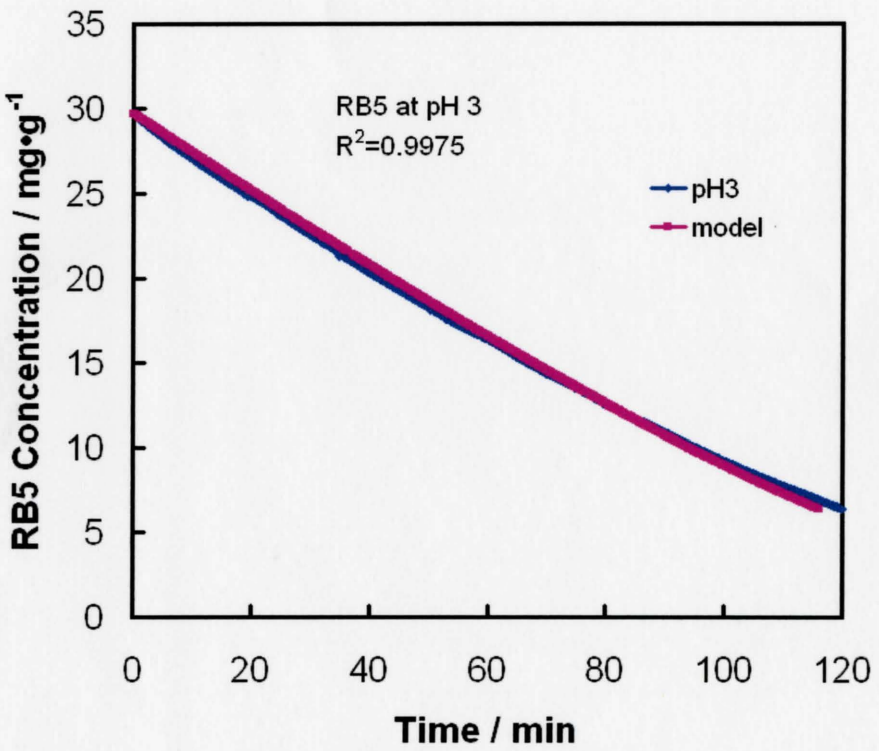

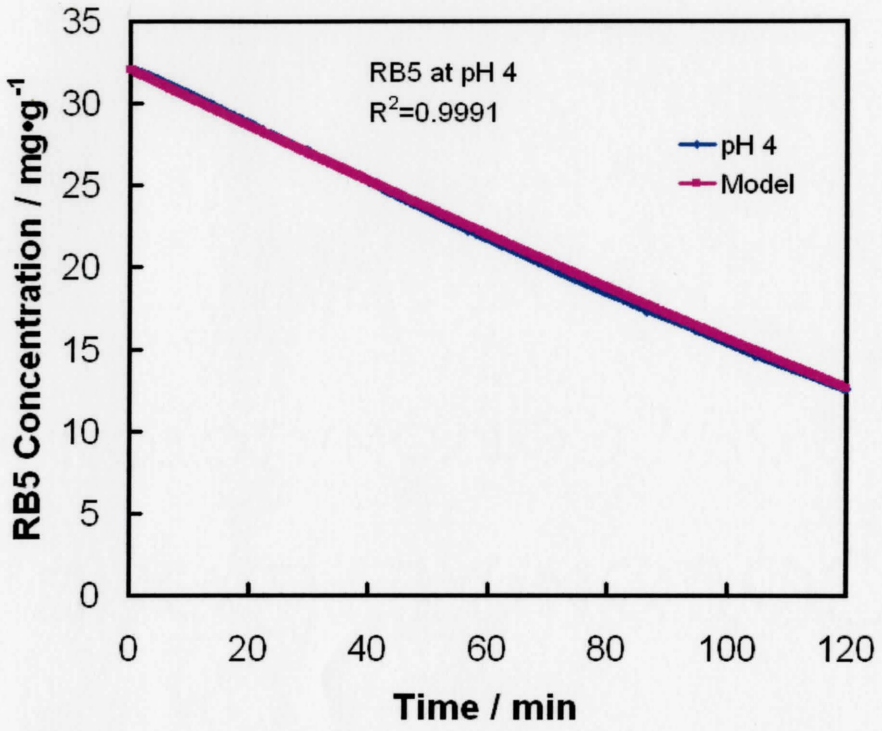
RB5 at pH 4
R^2=0.9991
pH 4
Model
RB5 Concentration / mg•g^{-1}
Time / min
0
5
10
15
20
25
30
35
0
20
40
60
80
100
120

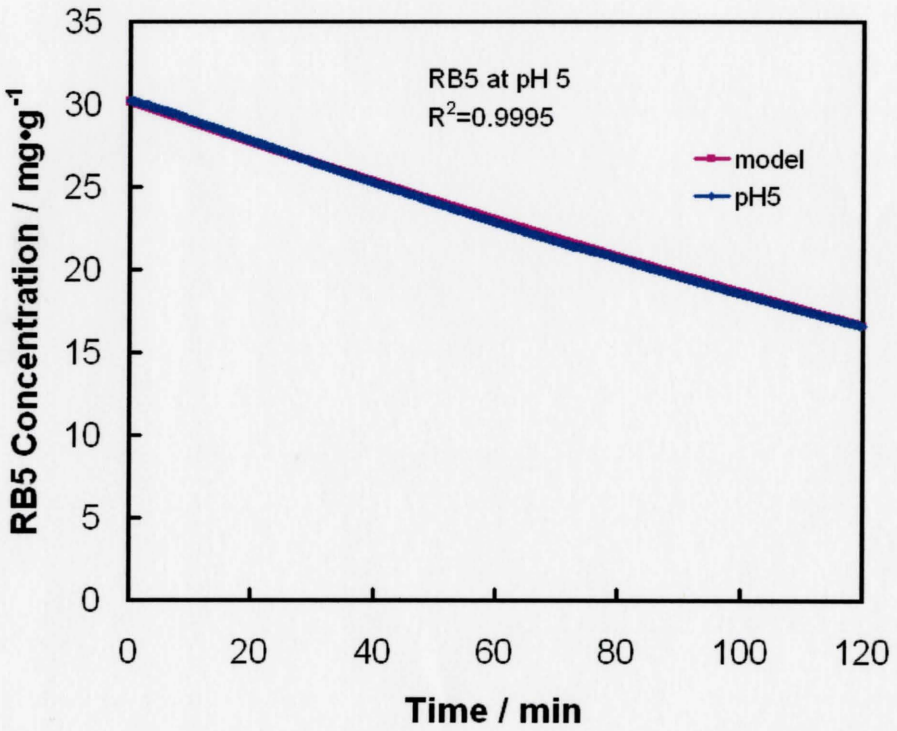
RB5 at pH 5
R^2=0.9995
model
pH5
RB5 Concentration / mg•g^{-1}
Time / min
0
5
10
15
20
25
30
35
0
20
40
60
80
100
120

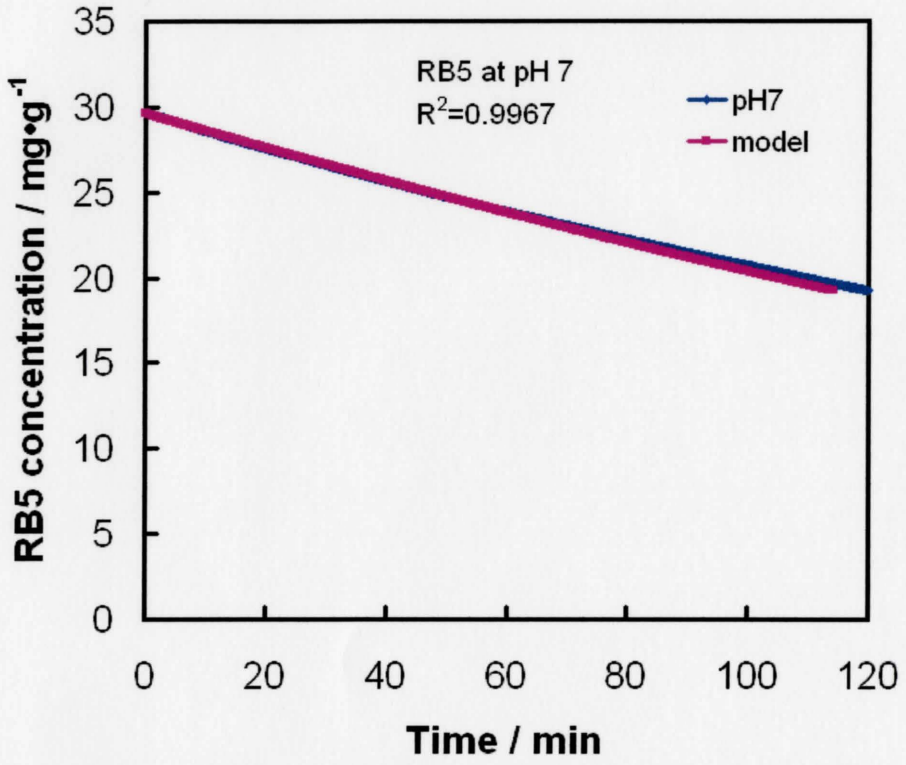

The fit is qualifiedly good. The results of k_1 are shown in Table 5.2

8 References

1. Liu, B. W.; Chou, M. S.; Kao, C. M.; Huang, B. J., Evaluation of selected operational parameters for the decolorization of dyefinishing wastewater using UV/ozone. *Ozone-Science & Engineering* **2004,** 26, (3), 239-245.

2. Oh, Y. K.; Kim, Y. J.; Ahn, Y.; Song, S. K.; Park, S., Color removal of real textile wastewater by sequential anaerobic and aerobic reactors. *Biotechnology and Bioprocess Engineering* **2004,** 9, (5), 419-422.

3. Aguedach, A.; Brosillon, S.; Morvan, J.; Lhadi, E. K., Photocatalytic degradation of azo-dyes reactive black 5 and reactive yellow 145 in water over a newly deposited titanium dioxide. *Applied Catalysis B: Environmental* **2005,** 57, (1), 55-62.

4. Guillard, C.; Lachheb, H.; Houas, A.; Ksibi, M.; Elaloui, E.; Herrmann, J.-M., Influence of chemical structure of dyes, of pH and of inorganic salts on their photocatalytic degradation by TiO2 comparison of the efficiency of powder and supported TiO2. *Journal of Photochemistry and Photobiology A: Chemistry* **2003,** 158, (1), 27-36.

5. Vandevivere, P. C.; Bianchi, R.; Verstraete, W., Treatment and reuse of wastewater from the textile wet-processing industry: Review of emerging technologies. *Journal of Chemical Technology and Biotechnology* **1998,** 72, (4), 289-302.

6. Bizani, E.; Fytianos, K.; Poulios, I.; Tsiridis, V., Photocatalytic decolorization and degradation of dye solutions and wastewaters in the presence of titanium dioxide. *Journal of Hazardous Materials* **2006,** 136, (1), 85-94.

7. Sarasa, J.; Roche, M. P.; Ormad, M. P.; Gimeno, E.; Puig, A.; Ovelleiro, J. L., Treatment of a wastewater resulting from dyes manufacturing with ozone and chemical coagulation. *Water Research* **1998,** 32, (9), 2721-2727.

8. Kusvuran, E.; Irmak, S.; Yavuz, H. I.; Samil, A.; Erbatur, O., Comparison of the treatment methods efficiency for decolorization and mineralization of Reactive Black 5 azo dye. *Journal of Hazardous Materials* **2005,** 119, (1-3), 109-116.

9. Sleiman, M.; Vildozo, D.; Ferronato, C.; Chovelon, J.-M., Photocatalytic degradation of azo dye Metanil Yellow: Optimization and kinetic modeling using a chemometric approach. *Applied Catalysis B: Environmental* **2007,** 77, (1-2), 1-11.

10. Karunakaran, C.; Dhanalakshmi, R., Photocatalytic performance of particulate semiconductors under natural sunshine--Oxidation of carboxylic acids. *Solar Energy Materials and Solar Cells* **2008,** 92, (5), 588-593.

11. Quintana, M.; Edvinsson, T.; Hagfeldt, A.; Boschloo, G., Comparison of Dye-Sensitized ZnO and TiO2 Solar Cells: Studies of Charge Transport and Carrier Lifetime. *J. Phys. Chem. C* **2007,** 111, (2), 1035-1041.

12. Chee, G.-J.; Nomura, Y.; Ikebukuro, K.; Karube, I., Development of photocatalytic biosensor for the evaluation of biochemical oxygen demand. *Biosensors and Bioelectronics* **2005,** 21, (1), 67-73.

13. Billik, P.; Plesch, G.; Brezov, V.; Kuchta, L.; Valko, M.; Mazur, M., Anatase TiO2 nanocrystals prepared by mechanochemical synthesis and their photochemical activity studied by EPR spectroscopy. *Journal of Physics and Chemistry of Solids* **2007,** 68, (5-6), 1112-1116.

14. Kozlova, E. A.; Vorontsov, A. V., Noble metal and sulfuric acid modified TiO2 photocatalysts: Mineralization of organophosphorous compounds. *Applied Catalysis B: Environmental* **2006,** 63, (1-2), 114-123.

15. Pelton, R.; Geng, X. L.; Brook, M., Photocatalytic paper from colloidal TiO2 - fact or fantasy. *Advances in Colloid and Interface Science* **2006,** 127, (1), 43-53.

16. Kormann, C.; Bahnemann, D. W.; Hoffmann, M. R., Photolysis of chloroform and other organic molecules in aqueous titanium dioxide suspensions. *Environmental Science and Technology* **1991,** 25, (3), 494-500.

17. Fox, M. A.; Dulay, M. T., Heterogeneous photocatalysis. *Chem. Rev.* **1993,** 93, (1), 341-357.

18. Stelzer, J. B.; Nitzsche, R.; Caro, J., Zeta potential measurement in catalyst preparations. *Chemical Engineering & Technology* **2005,** 28, (2), 182-186.

19. Hashimoto, K.; Irie, H.; Fujishima, A., TiO2 photocatalysis: A historical overview and future prospects. *Japanese Journal of Applied Physics, Part I: Regular Papers and Short Notes* **2005,** 44, (12), 8269-8285.

20. Fujishima, A.; Honda, K., Electrochemical photolysis of water at a semiconductor electrode. *Nature* **1972,** 238, (5358), 37-8.

21. Kawai, T.; Sakata, T., Conversion Of Carbohydrate Into Hydrogen Fuel By A Photocatalytic Process. *Nature* **1980,** 286, (5772), 474-476.

22. Kavan, L.; Gratzel, M.; Gilbert, S. E.; Klemenz, C.; Scheel, H. J., Electrochemical and Photoelectrochemical Investigation of Single-Crystal Anatase. *J. Am. Chem. Soc.* **1996,** 118, (28), 6716-6723.

23. Frank, S. N.; Bard, A. J., Heterogeneous photocatalytic oxidation of cyanide ion in aqueous solutions at titanium dioxide powder. *J. Am. Chem. Soc.* **1977,** 99, (1), 303-304.

24. Negishi, N.; Iyoda, T.; Hashimoto, K.; Fujishima, A., Preparation of transparent TiO2 thin-film photocatalyst and its photocatalytic activity. *Chemistry Letters* **1995,** (9), 841-842.

25. Tang, W. Z.; Huren, A., UV/TiO2 photocatalytic oxidation of commercial dyes in aqueous solutions. *Chemosphere* **1995,** 31, (9), 4157-4170.

26. Sauer, M. L.; Ollis, D. F., Photocatalyzed Oxidation of Ethanol and Acetaldehyde in Humidified Air. *Journal of Catalysis* **1996,** 158, (2), 570-582.

27. Khazraji, A. C.; Hotchandani, S.; Das, S.; Kamat, P. V., Controlling dye (Merocyanine-540) aggregation on nanostructured TiO2 films. An organized assembly approach for enhancing the efficiency of photosensitization. *Journal of Physical Chemistry B* **1999,** 103, (22), 4693-4700.

28. Augugliaro, V.; Coluccia, S.; Loddo, V.; Marchese, L.; Martra, G.; Palmisano, L.; Schiavello, M., Photocatalytic oxidation of gaseous toluene on anatase TiO2 catalyst: mechanistic aspects and FT-IR investigation. *Applied Catalysis B: Environmental* **1999,** 20, (1), 15-27.

29. Arslan, I.; Balcioglu, I. A., Degradation of commercial reactive dyestuffs by heterogenous and homogenous advanced oxidation processes: a comparative study. *Dyes and Pigments* **1999,** 43, (2), 95-108.

30. Mills, A.; Wang, J., Photobleaching of methylene blue sensitised by TiO2: an ambiguous system? *Journal of Photochemistry and Photobiology A: Chemistry* **1999,** 127, (1-3), 123-134.

31. Hsien, Y.-H.; Chang, C.-F.; Chen, Y.-H.; Cheng, S., Photodegradation of aromatic pollutants in water over TiO2 supported on molecular sieves. *Applied Catalysis B: Environmental* **2001,** 31, (4), 241-249.

32. Chen, C.; Li, X.; Ma, W.; Zhao, J.; Hidaka, H.; Serpone, N., Effect of Transition Metal Ions on the TiO2-Assisted Photodegradation of Dyes under Visible Irradiation: A Probe for the Interfacial Electron Transfer Process and Reaction Mechanism. *J. Phys. Chem. B* **2002,** 106, (2), 318-324.

33. Daneshvar, N.; Salari, D.; Khataee, A. R., Photocatalytic degradation of azo dye acid red 14 in water: investigation of the effect of operational parameters. *Journal of Photochemistry and Photobiology A: Chemistry* **2003,** 157, (1), 111-116.

34. Ku, Y.; Tseng, K. Y.; Ma, C. M., Photocatalytic decomposition of gaseous acetone using TiO2 and Pt/TiO2 catalysts. *International Journal of Chemical Kinetics* **2008,** 40, (4), 209-216.

35. Wold, A., Photocatalytic properties of TiO_2. *Chem. Mater.* **1993,** 5, 280-283.

36. Hoffmann, M. R.; Martin, S. T.; Choi, W.; Bahnemann, D. W., Environmental Applications of Semiconductor Photocatalysis. *Chem. Rev.* **1995,** 95, (1), 69-96.

37. Martin, S. T.; Herrmann, H.; Choi, W. Y.; Hoffmann, M. R., Time-resolved Microwave Conductivity. 1. TiO2 Photoractivity and size quantization. *Journal of the Chemical Society-Faraday Transactions* **1994,** 90, (21), 3315-3322.

38. Martin, S. T.; Herrmann, H.; Hoffmann, M. R., Time-Resolved Microwave Conductivity.2.Quantum-Sized TiO2 and The Effect of Adsorbates and Light-Intensity On Charge-Carrier Dynamics. *Journal of the Chemical Society-Faraday Transactions* **1994,** 90, (21), 3323-3330.

39. Tatsuma, T.; Tachibana, S.-i.; Fujishima, A., Remote Oxidation of Organic Compounds by UV-Irradiated TiO2 via the Gas Phase. *Journal of Physical Chemistry B* **2001,** 105, (29), 6987-6992.

40. Ishibashi, K.-i.; Fujishima, A.; Watanabe, T.; Hashimoto, K., Generation and Deactivation Processes of Superoxide Formed on TiO2 Film Illuminated by Very Weak UV Light in Air or Water. *Journal of Physical Chemistry B* **2000,** 104, (20), 4934-4938.

41. Nosaka, Y.; Kishimoto, M.; Nishino, J., Factors Governing the Initial Process of TiO2 Photocatalysis Studied by Means of in-Situ Electron Spin Resonance Measurements. *Journal of Physical Chemistry B* **1998,** 102, (50), 10279-10283.

42. Kamat, P. V., Photochemistry on nonreactive and reactive (semiconductor) surfaces. *Chem. Rev.* **1993,** 93, (1), 267-300.

43. Sun, L.; Bolton, J. R., Determination of the Quantum Yield for the Photochemical Generation of Hydroxyl Radicals in TiO2 Suspensions. *Journal of Physical Chemistry* **1996,** 100, (10), 4127-34.

44. Fox, M. A.; Abdelwahab, A. A., Photocatalytic Oxidation Of Multifunctional Organic-Molecules - The Effect Of An Intramolecular Aryl Thioether Group On The Semiconductor-Mediated Oxidation Dehydrogenation Of A Primary Aliphatic Alcohol. *Journal of Catalysis* **1990,** 126, (2), 693-696.

45. Samarghandi, M. R.; Nauri, J.; Mesdaghinia, A. R.; Mahvi, A.; Nasseri, S.; Vaezj, F., Efficiency removal of phenol, lead and cadmium by means of UV/TiO2/H2O2 processes. *International Journal of Environmental Science and Technology* **2007,** 4, (1), 19-25.

46. Aleboyeh, A.; Olya, M. E.; Aleboyeh, H., Electrical energy determination for an azo dye decolorization and mineralization by UV/H2O2 advanced oxidation process. *Chemical Engineering Journal* **2008,** 137, (3), 518-524.

47. Saquib, M.; Abu Tariq, M.; Faisal, M.; Muneer, M., Photocatalytic degradation of two selected dye derivatives in aqueous suspensions of titanium dioxide. *Desalination* **2008,** 219, (1-3), 301-311.

48. Kikuchi, Y.; Sunada, K.; Iyoda, T.; Hashimoto, K.; Fujishima, A., Photcatalytic bactericidal effect of TiO_2 thin films: dynamic view of the active oxygen species responsible for the effect. *Journal of Photochemistry and Photobiology, A: Chemistry* **1997,** 106.

49. Matsubara, H.; Takada, M.; Koyama, S.; Hashimoto, K.; Fujishima, A., Photoactive TiO2 containing paper: preparation and its photocatalytic activity under weak UV light illumination. *Chemistry Letters* **1995,** 9, 767-8.

50. Tsuge, Y.; Kim, J.; Sone, Y.; Kuwaki, O.; Shiratori, S., Fabrication of transparent TiO2 film with high adhesion by using self-assembly methods: Application to super-hydrophilic film. *Thin Solid Films* **2008,** 516, (9), 2463-2468.

51. Iguchi, Y.; Ichiura, H.; Kitaoka, T.; Tanaka, H., Preparation and characteristics of high performance paper containing titanium dioxide photocatalyst supported on inorganic fiber matrix. *Chemosphere* **2003,** 53, (10), 1193-1199.

52. Raillard, C.; Héquet, V.; Cloirec, P. L.; Legrand, J., Kinetic study of ketones photocatalytic oxidation in gas phase using TiO2-containing paper: effect of water vapor *Journal of Photochemistry and Photobiology, A: Chemistry* **2004,** 163, (3), 425-431.

53. Pichot, F.; Ferrere, S.; Pitts, R. J.; Gregg, B. A., Flexible solid-state photoelectrochromic windows. *Journal of the Electrochemical Society* **1999,** 146, (11), 4324-4326.

54. Arabatzis, I. M.; Antonaraki, S.; Stergiopoulos, T.; Hiskia, A.; Papaconstantinou, E.; Bernard, M. C.; Falaras, P., Preparation, characterization and photocatalytic activity of nanocrystalline thin film TiO2 catalysts towards 3,5-dichlorophenol degradation. *Journal of Photochemistry and Photobiology A: Chemistry* **2002,** 149, (1-3), 237-245.

55. Subramanian, M.; Vijayalakshmi, S.; Venkataraj, S.; Jayavel, R., Effect of cobalt doping on the structural and optical properties of TiO2 films prepared by sol-gel process. *Thin Solid Films* **2008,** 516, (12), 3776-3782.

56. Barka, N.; Assabbane, A.; Nounah, A.; Ichou, Y. A., Photocatalytic degradation of indigo carmine in aqueous solution by TiO2-coated non-woven fibres. *Journal of Hazardous Materials* **2008,** 152, (3), 1054-1059.

57. Junbo, Z.; Hong, Z.; Di, M.; An, L.; Minjiao, L.; Bin, X.; Jianzhang, L., Kinetic and anion degradation products study on photocatalytic degradation of reactive orange 5 solution with phosphotungstic acid. *Central European Journal of Chemistry* **2008,** 6, (1), 99-105.

58. Kumar, K. V.; Porkodi, K.; Rocha, F., Langmuir-Hinshelwood kinetics - A theoretical study. *Catalysis Communications* **2008,** 9, (1), 82-84.

59. Sopyan, I.; Watanabe, M.; Murasawa, S.; Hashimoto, K.; Fujishima, A., An efficient TiO2 thin-film photocatalyst: photocatalytic properties in gas-phase acetaldehyde degradation. *Journal of Photochemistry and Photobiology A: Chemistry* **1996,** 98, (1-2), 79-86.

60. Lachheb, H.; Puzenat, E.; Houas, A.; Ksibi, M.; Elaloui, E.; Guillard, C.; Herrmann, J.-M., Photocatalytic degradation of various types of dyes (Alizarin S, Crocein Orange G, Methyl Red, Congo Red, Methylene Blue) in water by UV-irradiated titania. *Applied Catalysis B: Environmental* **2002,** 39, (1), 75-90.

61. Tanaka, K.; Padermpole, K.; Hisanaga, T., Photocatalytic degradation of commercial azo dyes. *Water Research* **2000,** 34, (1), 327-333.

62. Tarasov, V. V.; Barancova, G. S.; Zaitsev, N. K.; Zhang, D. X., Photochemical Dinetics Of Organic Dye Oxidation In Water. *Process Safety and Environmental Protection* **2003,** 81, (B4), 243-249.

63. Julson, A. J.; Ollis, D. F., Kinetics of dye decolorization in an air-solid system. *Applied Catalysis B: Environmental* **2006,** 65, (3-4), 315-325.

64. Obee, T. N.; Brown, R. T., TiO2 Photocatalysis for Indoor Air Applications: Effects of Humidity and Trace Contaminant Levels on the Oxidation Rates of Formaldehyde, Toluene, and 1,3-Butadiene. *Environ. Sci. Technol.* **1995,** 29, (5), 1223-1231.

65. Tsoukleris, D. S.; Maggos, T.; Vassilakos, C.; Falaras, P., Photocatalytic degradation of volatile organics on TiO2 embedded glass spherules. *Catalysis Today* **2007,** 129, (1-2), 96-101.

66. Muruganandham, M.; Swaminathan, M., TiO2-UV photocatalytic oxidation of Reactive Yellow 14: Effect of operational parameters. *Journal of Hazardous Materials* **2006,** 135, (1-3), 78-86.

67. Egerton, T. A.; King, C. J., Influence of light-intensity on photoactivity in TiO2 Pigmented systems. *Journal of the Oil & Colour Chemists Association* **1979,** 62, (10), 386-391.

68. Ku, Y.; Lee, Y.-C.; Wang, W.-Y., Photocatalytic decomposition of 2-chlorophenol in aqueous solution by UV/TiO2 process with applied external bias voltage. *Journal of Hazardous Materials* **2006,** 138, (2), 350-356.

69. Bourikas, K.; Stylidi, M.; Kondarides, D. I.; Verykios, X. E., Adsorption of Acid Orange 7 on the Surface of Titanium Dioxide. *Langmuir* **2005,** 21, (20), 9222-9230.

70. Pelton, R., A model of the external surface of wood pulp fibers. *Nordic Pulp and Paper Research Journal* **1993,** 8, (1), 113-119.

71. D'Oliveira, J. C.; Al-Sayyed, G.; Pichat, P., Photodegradation of 2- and 3-chlorophenol in titanium dioxide aqueous suspensions. *Environ. Sci. Technol.* **1990,** 24, (7), 990-996.

72. Chen, D. W.; Ray, A. K., Photocatalytic kinetics of phenol and its derivatives over UV irradiated TiO2. *Applied Catalysis B-Environmental* **1999,** 23, (2-3), 143-157.

73. Chen, D.; Ray, A. K., Photodegradation kinetics of 4-nitrophenol in TiO2 suspension. *Water Research* **1998,** 32, (11), 3223-3234.

74. Matthews, R. W., Photooxidation of organic impurities in water using thin films of titanium dioxide. *J. Phys. Chem.* **1987,** 91, (12), 3328-3333.